

2023 1st Season Stock Assessment

Falkland calamari

(*Doryteuthis gahi*)



Andreas Winter

Natural Resources - Fisheries
Falkland Islands Government
Stanley, Falkland Islands

August 2023

S1 - 2023 - LOL



Index

Summary	2
Introduction.....	2
Methods.....	3
Stock assessment.....	7
Catch and effort.	7
Data.....	8
Group arrivals / depletion criteria.....	8
Depletion analyses.....	11
South.....	11
North.....	12
Immigration	14
Escapement biomass.....	15
Fishery bycatch	16
Trawl area coverage.....	18
References.....	20
Appendix.....	24
<i>Doryteuthis gahi</i> individual weights.....	24
Prior estimates and CV	25
Depletion model estimates and CV	26
Combined Bayesian models	27
Natural mortality.....	29
Total catch by species.....	30

Summary

- The 2023 first season *Doryteuthis gahi* fishery (C license) was open from February 26th and closed on schedule April 30th. Compensatory flex days resulted in fifteen vessel-days, by eight vessels, taken after April 30th, with the last three vessels fishing until May 3rd.
- 52,704 tonnes *D. gahi* catch was reported in the 2023 C-license fishery, giving an average CPUE of 54.2 t vessel-day⁻¹. Total catch and CPUE were second-lowest among the most recent 5 first seasons. 42.7% of *D. gahi* catch and 46.0% of fishing effort were taken south of 52° S; 57.3% of *D. gahi* catch and 54.0% of fishing effort were taken north of 52° S.
- In the south sub-area, four depletion periods / immigration peaks were inferred on February 26th (start of the season), March 21st, April 6th, and April 26th. In the north sub-area, four depletion periods / immigrations were inferred on February 26th, March 5th, March 25th, and April 24th.
- Approximately 116,360 tonnes of *D. gahi* (95% confidence interval: 112,010 to 278,697 t) were estimated to have immigrated into the Loligo Box after the start of first season 2023, of which 49,410 t in the south sub-area and 66,950 t in the north sub-area.
- The escapement biomass estimate for *D. gahi* remaining in the Loligo Box at the end of first season 2023 was: Maximum likelihood 57,647 tonnes, with a 95% confidence interval of 56,315 to 185,125 tonnes.
The risk of *D. gahi* escapement biomass at the end of the season being less than 10,000 tonnes was estimated at effectively zero.

Introduction

First season (C licence) of the 2023 *Doryteuthis gahi* fishery (Patagonian longfin squid – colloquially *Loligo*) opened on February 26th (FIG 2023). Throughout the season, 16 compensatory days were requested by ten of the vessels, of which six on one day: March 28th. A total of 15 fishing days were taken after scheduled closure on April 30th with the last three vessels fishing on May 3rd.

All C-licensed vessels were required to embark a Marine Mammal Observer to monitor presence and incidental capture of pinnipeds, and as now standard protocol, seal exclusion devices (SEDs) were mandatory for the duration of the season. Ultimately, 2 pinniped mortalities and 19 live releases were reported for the season: 2 (15) South American fur seals *Arctocephalus australis*, and 0 (4) Southern sea lions *Otaria flavescens*.

Total reported *D. gahi* catch under first season C licence was 22,525.5 south + 30,178.8 north = 52,704.4 tonnes, corresponding to an average CPUE of $52704 / 972 = 54.2$ tonnes vessel-day⁻¹. Both total catch and average CPUE were second-lowest among the most recent five first seasons (2019 to 2023), although well above long-term averages (Table 1).

Assessment of the Falkland Islands *D. gahi* stock was conducted with depletion time-series models as in previous seasons (Agnew et al. 1998, Arkhipkin et al. 2008, Winter and Arkhipkin 2015), and in other squid fisheries (cited in Arkhipkin et al. 2021). Because *D. gahi* has an annual life cycle (Patterson 1988, Arkhipkin 1993), stock cannot be derived from a standing biomass carried over from prior years (Rosenberg et al. 1990, Pierce and Guerra 1994). The depletion model instead calculates an estimate of population abundance over time by evaluating what levels of abundance and catchability must be present to sustain the observed rate of catch. Depletion modelling of the *D. gahi* target fishery is used in-season, for projection, and for post-season analysis, with the objective of maintaining an escapement biomass of 10,000 tonnes *D. gahi* at the end of each season as a conservation threshold (Agnew et al. 2002, Barton 2002).

Table 1. *D. gahi* season comparisons since 2004, when catch management was assumed by the FIFD. Days: total number of calendar days open to licensed *D. gahi* fishing including (since 1st season 2013) optional flex days; V-Days: aggregate number of licensed *D. gahi* fishing days reported by all vessels for the season. Entries in italics are seasons closed by emergency order.

	Season 1			Season 2		
	Catch (t)	Days	V-Days	Catch (t)	Days	V-Days
2004	7,152	46	625	17,559	78	1271
2005	24,605	45	576	29,659	78	1210
2006	19,056	50	704	23,238	53	883
2007	17,229	50	680	24,171	63	1063
2008	24,752	51	780	26,996	78	1189
2009	12,764	50	773	17,836	59	923
2010	28,754	50	765	36,993	78	1169
2011	15,271	50	771	18,725	70	1099
2012	34,767	51	770	35,026	78	1095
2013	19,908	53	782	19,614	78	1195
2014	28,119	59	872	19,630	71	1099
2015	19,383	57	871 ^A	10,190	42	665
2016	22,616	68	1020	23,089	68	1004
2017	39,433	68	999 ^B	24,101	69	1002 ^C
2018	43,085	69	975	35,828	68	977
2019	55,586	68	953	24,748	43	635
2020	29,116	68	1012	29,759	69	993
2021	59,587	62	891	34,750	68	982 ^D
2022	56,417	68	966 ^E	43,216	68	982
2023	52,704	67	972			

^A Does not include C-license catch or effort after the target was switched from *D. gahi* to *Illex*.

^B Includes two vessel-days of experimental fishing for juvenile toothfish.

^C Includes one vessel-day of experimental fishing for juvenile toothfish.

^D Includes three vessel-days of experimental fishing for SED improvement.

^E Includes three vessel-days of exploratory fishing north of the Loligo Box.

Methods

The depletion model formulated for the Falklands *D. gahi* stock is based on the equivalence:

$$C_{\text{day}} = q \times E_{\text{day}} \times N_{\text{day}} \times e^{-M/2} \quad (1)$$

where q is the catchability coefficient, M is the natural mortality rate (considered constant at 0.0133 day^{-1} ; see Appendix – Natural mortality), and C_{day} , E_{day} , N_{day} are respectively catch (numbers of squid), fishing effort (numbers of vessels), and abundance (numbers of squid) per day. The catchability coefficient q summarized the range of variation of all trawls taken by the fishing fleet in this season.

In its basic form (DeLury 1947) the depletion model assumes a closed population in a fixed area for the duration of the assessment. However, the assumption of a closed population is imperfectly met in the Falkland Islands fishery, where stock analyses have often shown that *D. gahi* groups arrive in successive waves after the start of the season (Arkhipkin et al. 2021). Arrivals of successive groups are inferred from discontinuities in the catch data. Fishing on a single, closed cohort would be expected to yield gradually decreasing CPUE, but gradually

increasing average individual sizes, as the squid grow. When instead these data change suddenly, or in contrast to expectation, the immigration of a new group to the population is indicated (Winter and Arkhipkin 2015).

In the event of a new group arrival, the depletion calculation must be modified to account for this influx. Modification is done using a simultaneous algorithm that adds new arrivals on top of the stock previously present, and posits a common catchability coefficient for the entire depletion time-series. If two depletions are included in the same model (i.e., the stock present from the start plus a new group arrival), then:

$$C_{\text{day}} = q \times E_{\text{day}} \times (N1_{\text{day}} + (N2_{\text{day}} \times i2|_0^1)) \times e^{-M/2} \quad (2)$$

where $i2$ is a dummy variable taking the values 0 or 1 if ‘day’ is before or after the start day of the second depletion. For more than two depletions, $N3_{\text{day}}$, $i3$, $N4_{\text{day}}$, $i4$, etc., would be included following the same pattern.

The season depletion likelihood function was calculated as the difference between actual catch numbers reported and catch numbers predicted from the model (Equation 2), statistically corrected by a factor relating to the number of days of the depletion period (Roa-Ureta 2012):

$$\text{minimization} \rightarrow ((n\text{Days} - 2)/2) \times \log\left(\sum_{\text{days}} \left(\log(\text{predicted } C_{\text{day}}) - \log(\text{actual } C_{\text{day}})\right)^2\right) \quad (3)$$

The stock assessment was set in a Bayesian framework (Punt and Hilborn 1997), whereby results of the season depletion model are conditioned by prior information on the stock; in this case the information from the pre-season survey.

The likelihood function of prior information was calculated as the normal distribution of the difference between catchability derived from the survey abundance estimate ($_{\text{prior}} q$), and catchability derived from the season depletion model ($_{\text{depletion}} q$). Applying this difference requires both the survey and the season to be fishing the same stock with the same gear. Catchability, rather than abundance N , is used for calculating prior likelihood because catchability informs the entire season time series; whereas N from the survey only informs the first in-season depletion period – subsequent immigrations and depletions are independent of the abundance that was present during the survey. Thus, the prior likelihood function was:

$$\text{minimization} \rightarrow \frac{1}{\sqrt{2\pi \cdot SD_{\text{prior } q}^2}} \times \exp\left(-\frac{(\text{depletion } q - \text{prior } q)^2}{2 \cdot SD_{\text{prior } q}^2}\right) \quad (4)$$

where the standard deviation of catchability prior ($SD_{\text{prior } q}$) was calculated from the Euclidean sum (Carlson 2014) of the survey prior estimate uncertainty, the variability in catches on the season start date, and the uncertainty in the natural mortality M estimate over the number of days mortality discounting (Appendix Equation A5).

Bayesian optimization of the depletion was calculated by jointly minimizing Equations 3 and 4, using the Nelder-Mead algorithm in R programming package ‘optimx’ (Nash and Varadhan 2011). Relative weights in the joint optimization were assigned to Equations 3 and 4 as the converse of their coefficients of variation (CV), i.e., the CV of the prior became the weight of the depletion model and the CV of the depletion model became the weight of the prior. Calculations of the depletion CVs are described in Equations A8-S and A8-N. Because a complex model with multiple depletions may converge on a local minimum rather than global minimum, the optimization was stabilized by running a feed-back loop that set the q and N

parameter outputs of the Bayesian joint optimization back into the in-season-only minimization (Equation 3), re-calculated the in-season-only minimization, then re-calculated the Bayesian joint optimization, and continued this process until both the in-season minimization and the joint optimization remained unchanged.

With actual C_{day} , E_{day} and M being fixed parameters, the optimization of Equation 2 using Equations 3 and 4 produces estimates of q and N_1, N_2, \dots , etc. Numbers of squid on the final day (or any other day) of a time series are then calculated as the numbers N of the depletion start days discounted for natural mortality during the intervening period, and subtracting cumulative catch also discounted for natural mortality (CNMD). Taking for example a two-depletion period:

$$N_{\text{final day}} = N_1_{\text{start day 1}} \times e^{-M(\text{final day} - \text{start day 1})} + N_2_{\text{start day 2}} \times e^{-M(\text{final day} - \text{start day 2})} - \text{CNMD}_{\text{final day}}, \quad (5)$$

$$\text{CNMD}_{\text{day 1}} = 0$$

$$\text{CNMD}_{\text{day x}} = \text{CNMD}_{\text{day x-1}} \times e^{-M} + C_{\text{day x-1}} \times e^{-M/2} \quad (6)$$

$N_{\text{final day}}$ is then multiplied by the average individual weight of squid on the final day to give biomass. Daily average individual weight is obtained from length / weight conversion of mantle lengths measured in-season by observers, and also derived from in-season commercial data as the proportion of product weight that vessels reported per market size category^a. Observer mantle lengths are scientifically more accurate, but restricted to a partial sample of trawls. Commercially proportioned mantle lengths are relatively less accurate, but cover every trawl of the entire fishing fleet every day. Therefore, both sources of data are used (see Appendix – *Doryteuthis gahi* individual weights).

Distributions of the likelihood estimates from joint optimization (i.e., measures of their statistical uncertainty) were computed using a Markov Chain Monte Carlo (MCMC) (Gelman and Lopes 2006), a method that is commonly employed for fisheries assessments (Magnusson et al. 2013). MCMC is an iterative process which generates random stepwise changes to the proposed outcome of a model (in this case, the q and N of *D. gahi* squid) and at each step, accepts or nullifies the change with a probability equivalent to how well the change fits the model parameters compared to the previous step. The resulting sequence of accepted or nullified changes (i.e., the ‘chain’) approximates the likelihood distribution of the model outcome. The MCMC of the depletion models were run for 200,000 iterations; the first 1000 iterations were discarded as burn-in sections (initial phases over which the algorithm stabilizes); and the chains were thinned by a factor equivalent to the maximum of either 5 or the inverse of the acceptance rate (e.g., if the acceptance rate was 12.5%, then every eighth (0.125^{-1}) iteration was retained) to reduce serial correlation. For each model three chains were run; one chain initiated with the parameter values obtained from the joint optimization of Equations 3 and 4, one chain initiated with these parameters $\times 2$, and one chain initiated with these parameters $\times 1/4$. Convergence of the three chains was accepted if the variance among chains was less than 10% higher than the variance within chains (Brooks and Gelman 1998). When convergence was satisfied the three chains were combined as one final set. Equations 5, 6, and the multiplication by average individual weight were applied to the CNMD and to each iteration of N values in the final set, and the biomass outcomes from these calculations represent the distribution of the estimate.

^a First reported for Falkland Islands *D. gahi* by Payá (2006). Also used in some finfish commercial fisheries, see Plet-Hansen et al. 2018.

Depletion models and likelihood distributions were calculated separately for north and south sub-areas of the Loligo Box fishing zone (Figure 1), as *D. gahi* sub-stocks emigrate from different spawning grounds and remain to an extent segregated (Arkhipkin and Middleton 2002), although they represent a single intermixed population (Shaw et al. 2004). However, q_{prior} was calculated for the north and south sub-areas combined, rather than separately (Equation A4). As fishing tends to start predominantly in one or the other sub-area, rather than the fleet spreading itself evenly, separately computed north and south q_{prior} are susceptible to arbitrary differences. Total escapement biomass was then defined as the aggregate biomass of *D. gahi* on the last day of the season for north and south sub-areas combined, with north and south likelihood distributions added together randomly.

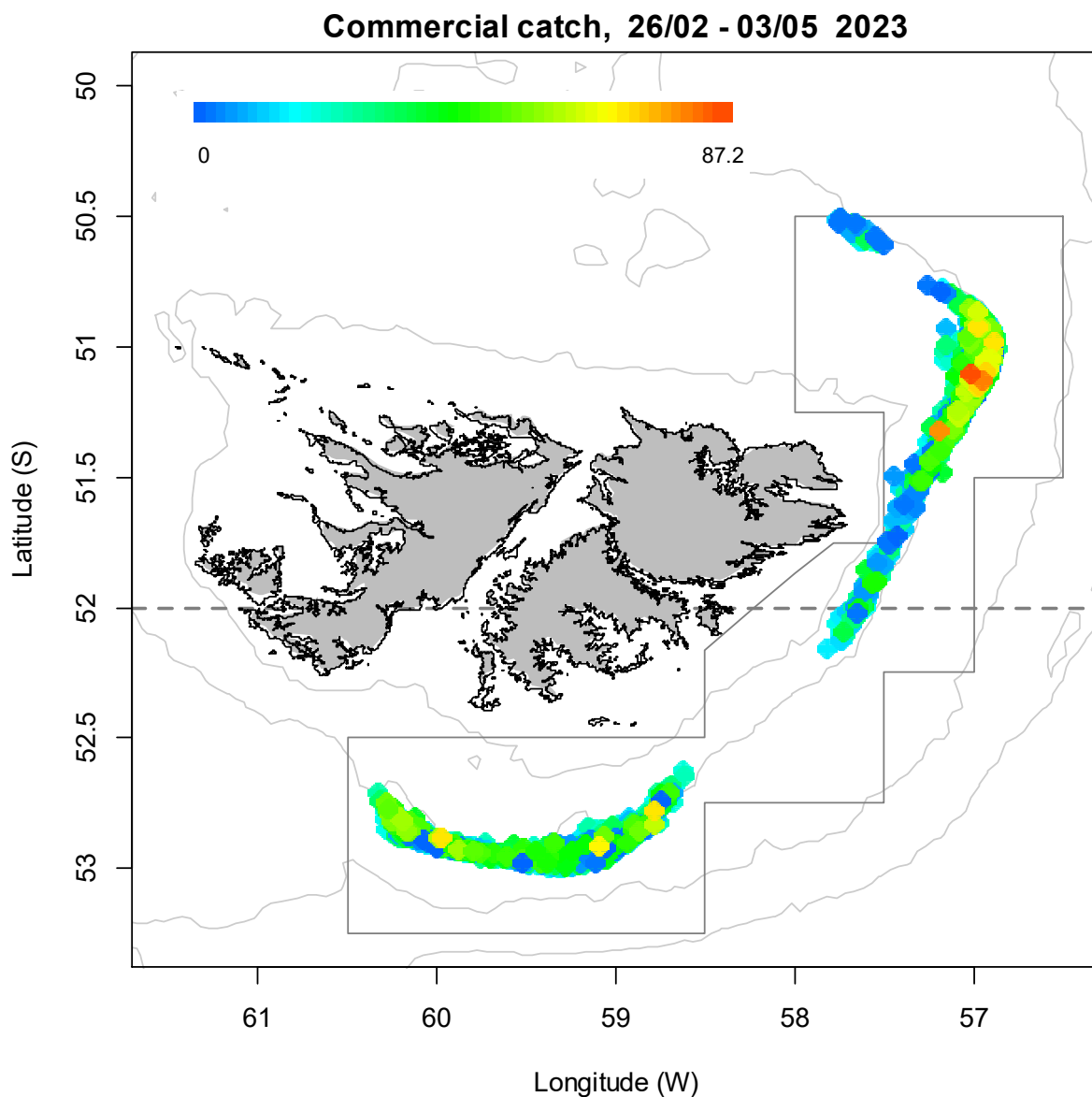


Figure 1. Spatial distribution of *D. gahi* first-season trawls (mean coordinate positions), colour-scaled to catch weight (max. = 87.2 tonnes). 2283 trawl catches were taken during the season. The Loligo Box fishing zone and 52 °S parallel delineating the boundary between north and south assessment sub-areas, are shown in grey.

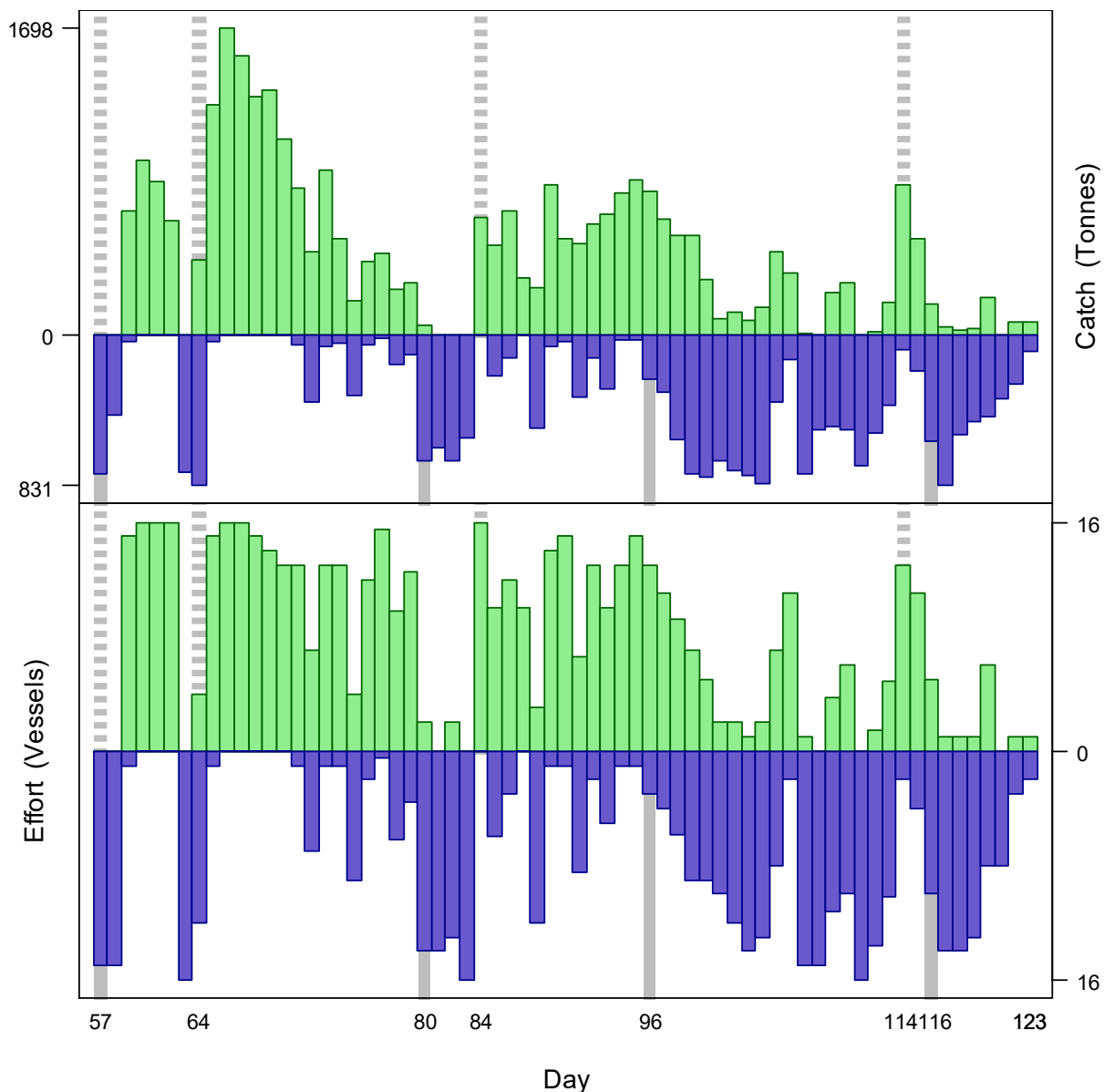


Figure 2. Daily total *D. gahi* catch and effort distribution by assessment sub-area north (green) and south (purple) of the 52° S parallel during first season 2023. The season was open from February 26th (chronological day 57) with directed closure on April 30th (day 120), and flex days until May 3rd (day 123). As many as 16 vessels fished per day north; as many as 16 vessels fished per day south. As much as 1698 tonnes *D. gahi* was caught per day north; as much as 831 t *D. gahi* was caught per day south.

Stock assessment Catch and effort

The north sub-area was fished on 59 of 67 season-days, for 57.3% of total catch (30178.8 tonnes *D. gahi*) – the highest percentage for a first season since 2018 and 54.0% of effort (524.7 vessel-days) (Figures 1 and 2). The south sub-area was fished on 57 of the 67 season-days, for 42.7% of total catch (22525.5 t *D. gahi*) and 46.0% of effort (447.3 vessel-days). The centre ‘square’ of the Loligo Box; between 58.5° to 57.5° W longitude and 52.25° to 52.75° S latitude, being completely unfished (Figure 1) is unprecedented since at least 2010, although the general pattern of sparse fishing in this square is not unusual. In first season 2019 only 1 of 2685 trawls

was taken in this square (Winter 2019a), in first season 2021 only 4 of 2341 trawls (Winter 2021), and in first season 2022 only 3 of 2445 trawls (Winter and Skeljo 2022).

Data

972 vessel-days were fished during the season (Table 1), with a median of 15 vessels per day (mean 14.51). Vessels reported daily catch totals to the FIFD and electronic logbook data that included trawl times, positions, depths, and product weight by market size categories. Four FIG fishery observers were deployed on four vessels in the fishing season for a total of 57 sampling days^b (Peruzzo 2023, Amukwaya 2023, Nicholls 2023, Fournier-Carnoy 2023). Throughout the 67 days of the season, 18 days had no FIG fishery observer sampling, 41 days had 1 FIG fishery observer sampling, and 8 days had two FIG fishery observers sampling. Except for seabird days FIG fishery observers were tasked with sampling 200 *D. gahi* at two stations daily; reporting their maturity stages, sex, and lengths to 0.5 cm. Contract marine mammal observers were tasked with measuring 100 unsexed lengths of *D. gahi* per day. The length-weight relationship for converting observer and commercially proportioned lengths was combined from first pre-season and season length-weight data of both 2022 and 2023, as 2023 data became available progressively with on-going observer coverage. The final parameterization of the length-weight relationship included 5821 measures from 2022 and 6974 measures from 2023, giving:

$$\text{weight (kg)} = 0.13556 \times \text{length (cm)}^{2.31464} / 1000 \quad (7)$$

with a coefficient of determination $R^2 = 92.2\%$.

Group arrivals / depletion criteria

Start days of depletions - following arrivals of new *D. gahi* groups - were judged primarily by daily changes in CPUE, with additional information from sex proportions, maturity, and average individual squid sizes. CPUE was calculated as metric tonnes of *D. gahi* caught per vessel per day. Days were used rather than trawl hours as the basic unit of effort. Commercial vessels do not trawl standardized duration hours, but rather durations that best suit their daily processing requirements. An effort index of days is therefore more consistent (FIFD 2004, Winter and Arkhipkin 2015). Inclusion of additional depletion starts was partially evaluated by improvement of the Akaike information criterion (AIC; Akaike 1973) on model fit.

Four days south and four days north were identified that represented the onset of significant immigrations / depletions throughout the season. One additional day in each of the north and south was evaluated for having either a CPUE peak or marked changes in biological indicators, but ultimately these days did not show substantiated influence on the depletion models, by improvement of the AIC. The last two days of fishing both north and south also had high CPUE (Figure 4), but were considered ‘fill-up’ catches by the few remaining vessels and not further immigration events.

- The first depletion start south was set by definition on day 57 (February 26th), the first day of the season with all fifteen vessels fishing south. CPUE on that day was moderately high (Figure 4), the proportion of females was near the highest of the season (Figure 5C), and average male maturities were near lowest of the season (Figure 5D).

^b Not counting seabird days (every fourth day).

- The second depletion start south was identified on day 80 (March 21st), as CPUE increased sharply after a period of decline (Figure 4), and the proportion of females was markedly higher after several low days (Figure 5C).
- The third depletion start south was identified on day 96 (April 6th), as CPUE increased to the highest level of the season (Figure 4), average individual observer weights started an increasing trend (Figure 5B), and the proportion of females was the lowest of the season (Figure 5C).
- The fourth depletion start south was identified on day 116 (April 26th) as CPUE rose to the highest level in 10 days (Figure 4), while the proportion of females decreased to a local minimum (Figure 5C) and average individual commercial weight, average individual observer weights, and average maturities all showed increasing trends (Figure 5A, 5B, 5D).
- The first depletion start north was set by definition on day 57 (February 26th), although no fishing in the north occurred until two days later. The average proportion of females in the north shortly after day 57 was the highest of the season (Figure 5C).
- The second depletion start north was identified on day 64 (March 5th), with a peak in CPUE (Figure 4), the highest average individual commercial weight (Figure 5A), and the highest unsexed average individual observer weight (Figure 5B) of the season.
- The third depletion start north was identified on day 84 (March 25th), the first time in five days that more than two vessels fished in the north (Figure 4), and the highest male and female average maturities up to that date in the season (Figure 5D).
- The fourth depletion start north was identified on day 114 (April 24th), with a peak in CPUE (Figure 4), and the highest proportion of females recorded in over three weeks (Figure 5C).

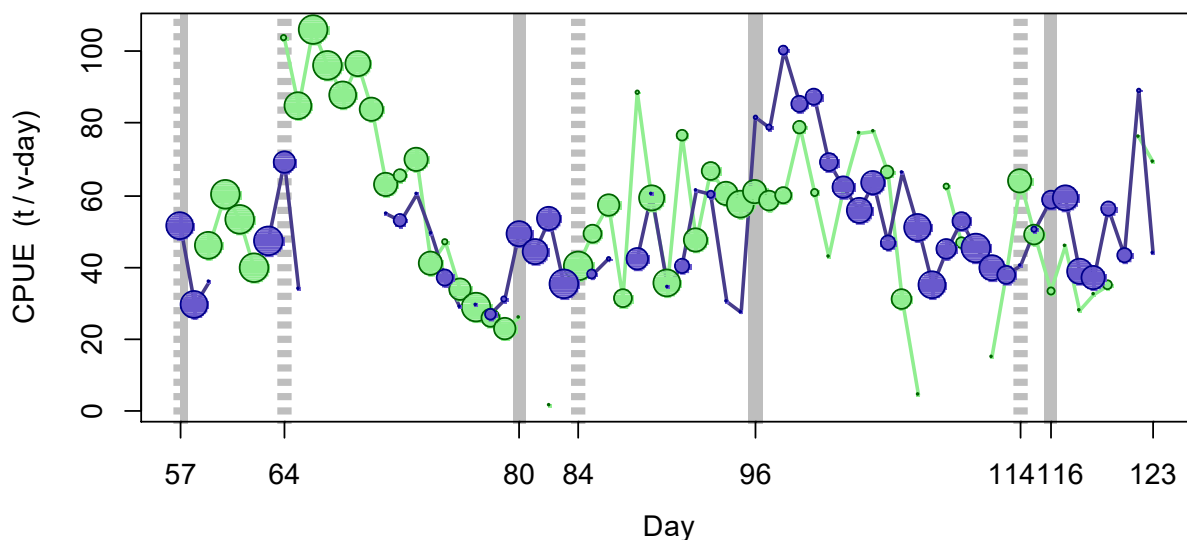


Figure 4. CPUE in metric tonnes per vessel per chronological day, by assessment sub-area north (green) and south (purple) of 52° S latitude. Circle sizes are proportioned to numbers of vessels fishing. Data from consecutive days are joined by line segments. Broken grey bars indicate the starts of in-season depletions north. Solid grey bars indicate the starts of in-season depletions south.

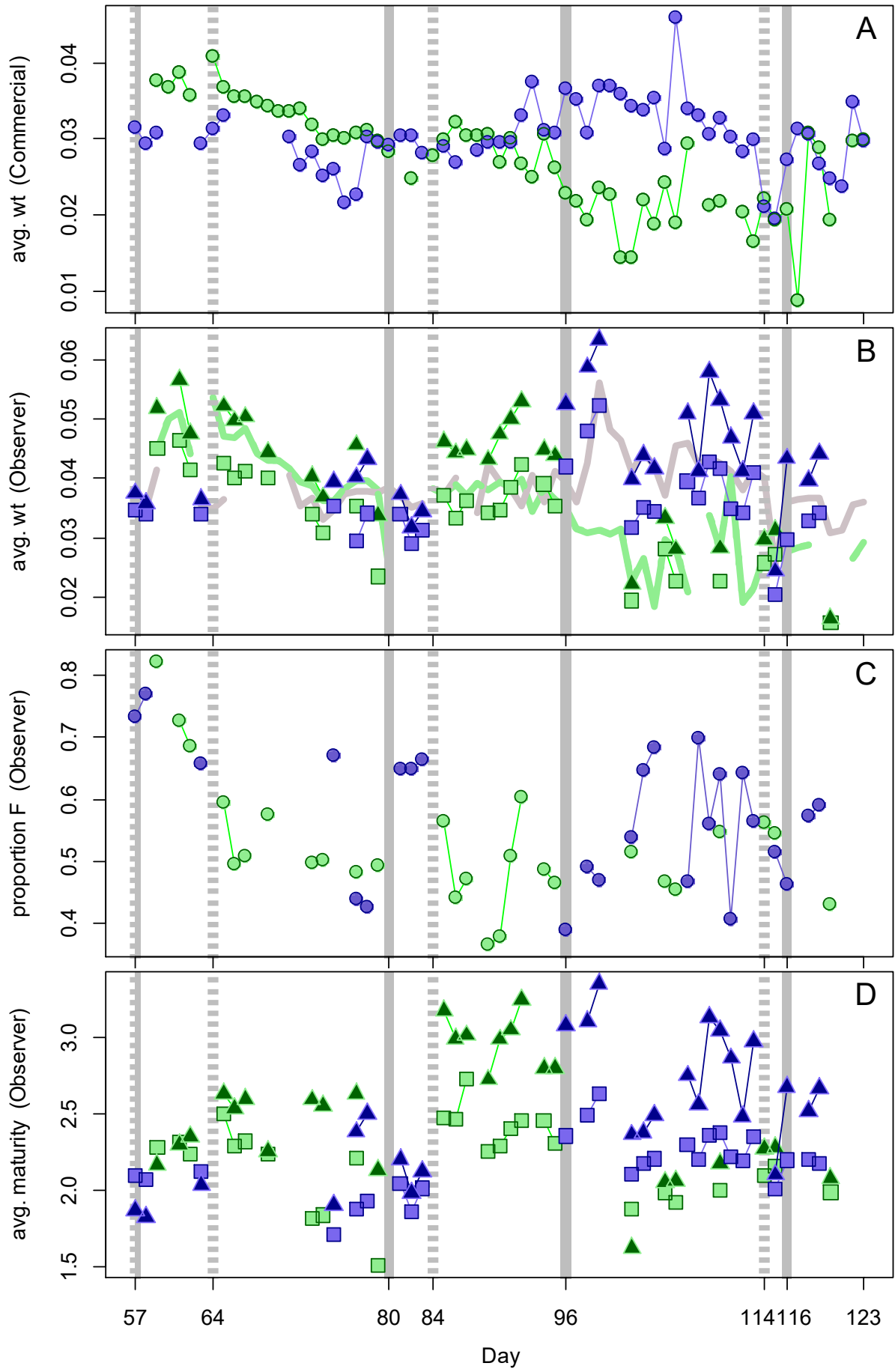


Figure 5 [previous page]. A: Average individual *D. gahi* weights (kg) per day from commercial size categories. B: Average individual *D. gahi* weights (kg) by sex per day from FIG observer sampling. C: Proportions of female *D. gahi* per day from observer sampling. D: Average maturity index value (Lipiński 1979) by sex per day from observer sampling. Males: triangles, females: squares, combined: circles. Thick lines (B) are unsexed measurements from the contract marine mammal observers. North sub-area: green, south sub-area: purple. Data from consecutive days are joined by line segments. Broken grey bars: starts of in-season depletions north. Solid grey bars: starts of in-season depletions south.

Depletion analyses

South

In the south sub-area, the maximum likelihood posterior ($\text{Bayesian } q_S = 1.443 \times 10^{-3}$; Figure 5-left, and Equation A9-S) was centred between the prior ($\text{prior } q = 1.272 \times 10^{-3}$; Figure 5-left, and Equation A4) and the in-season depletion ($\text{depletion } q_S = 1.802 \times 10^{-3}$; Figure 5-left, and Equation A6-S). CV of the prior was about $4\times$ higher than CV of the in-season depletion (Equations A5 and A8-S), but in any case, the MCMC distribution of the posterior showed a very skewed model fit with a modal peak far different from the empirical $\text{Bayesian } q_S$. Actual depletion throughout the time series had been inconsistent (Figure 4).

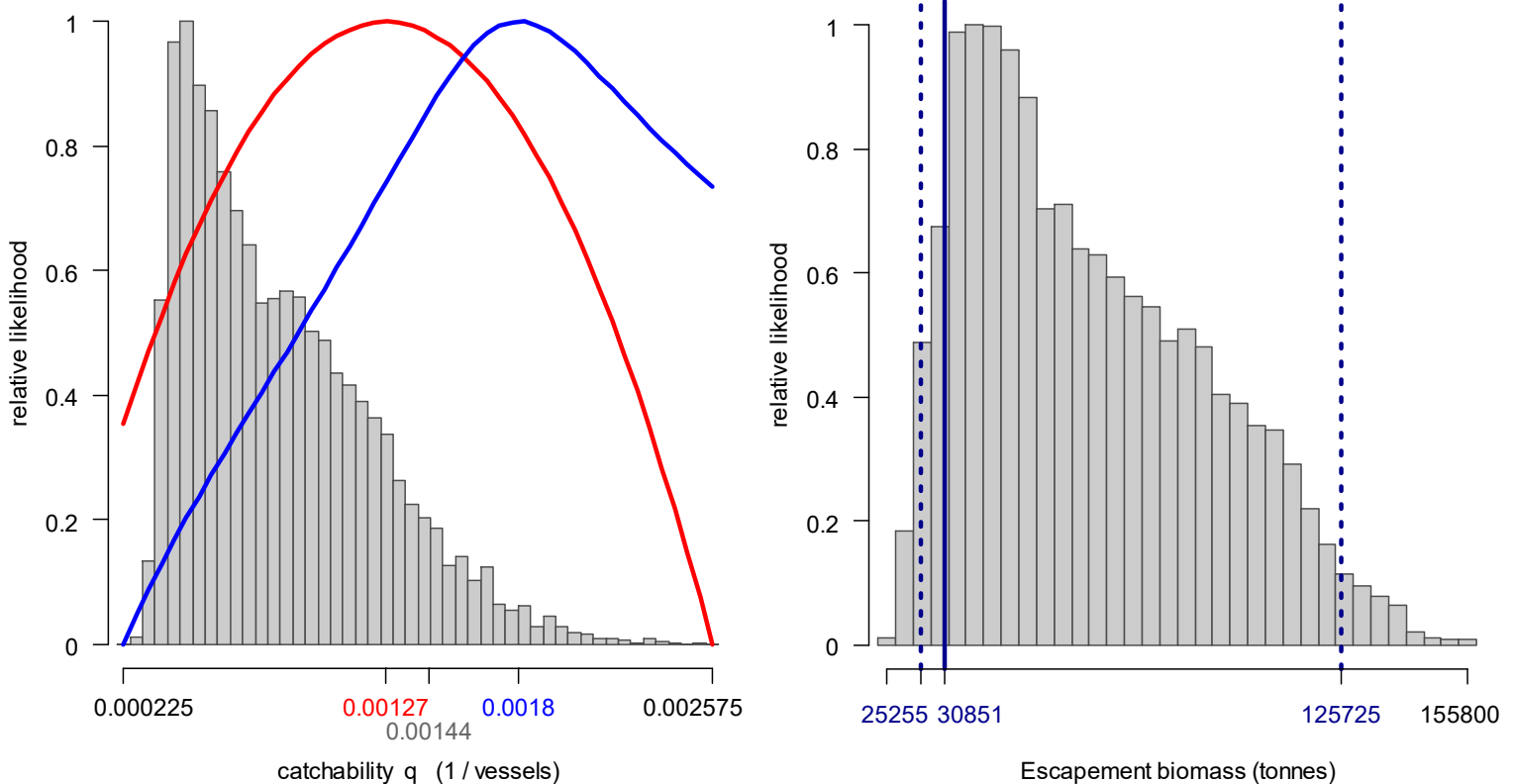


Figure 5. South sub-area. Left: Likelihood distributions for *D. gahi* catchability. Red line: prior model (pre-season survey data), blue line: in-season depletion model, grey bars: combined Bayesian model posterior. Right: Likelihood distribution (grey bars) of escapement biomass, from Bayesian posterior and average individual squid weight at the end of the season. Blue lines: maximum likelihood and 95% confidence interval. Note correspondence to Figure 6.

The MCMC distribution of the Bayesian posterior multiplied by the generalized additive model (GAM) fit of average individual squid weight (Figure A1-south) gave the likelihood distribution of *D. gahi* biomass on day 123 (May 3rd) shown in Figure 5-right, with maximum likelihood and 95% confidence interval of:

$$B_{S \text{ day } 123} = 30,851 \text{ t} \sim 95\% \text{ CI } [25,255 - 125,725] \text{ t} \quad (8-S)$$

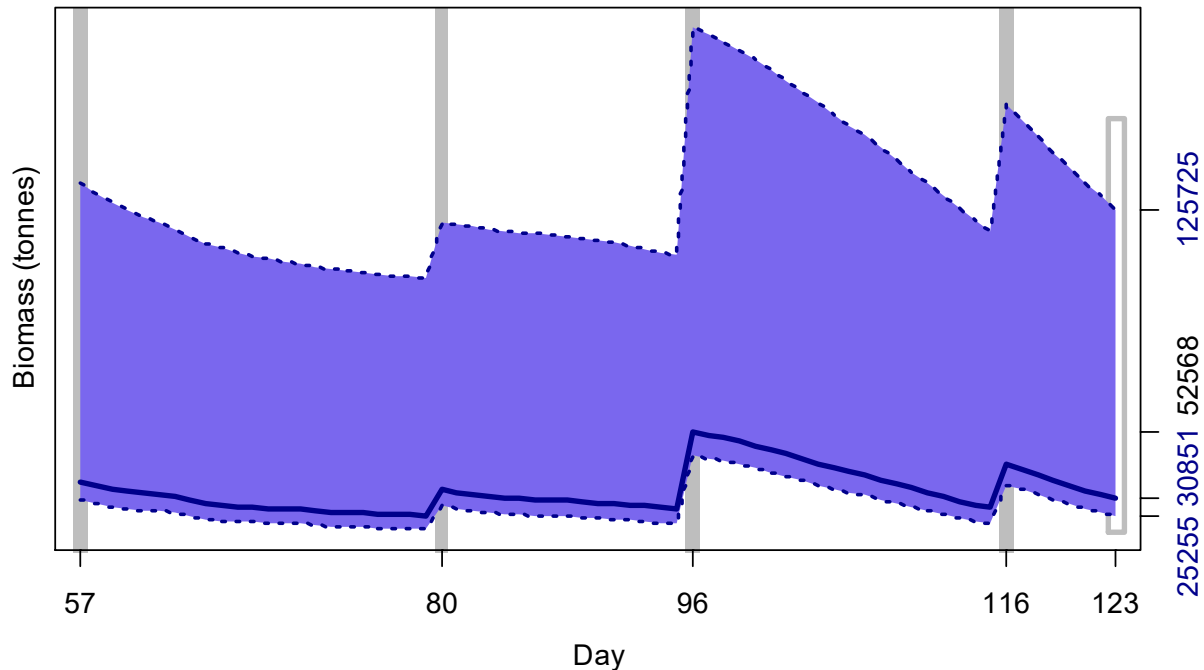


Figure 6. South sub-area. *D. gahi* biomass time series estimated from Bayesian posterior of the depletion model \pm 95% confidence interval. Grey bars indicate the start of in-season depletions south; days 57, 80, 96, and 116. Note that the biomass ‘footprint’ on day 123 (May 3rd) corresponds to the right-side plot of Figure 5.

On the first day of the season estimated *D. gahi* biomass south was 36,215 t \sim 95% CI [30,414 – 134,449] t (Figure 6); given the high margin of error not statistically different ($p > 0.09$) from the pre-season estimate of 26,675 t [24,725 – 60,815] (Winter et al. 2023). The highest biomass estimate of the season occurred with the 2nd immigration on day 96, reaching 52,568 t [44,749 – 185,494]. Effectively, the variation of biomass estimate throughout the season was not statistically significant; by the rule that a straight line could be drawn through the plot (Figure 6) without intersecting the 95% confidence interval (Swartzman et al. 1992).

North

In the north sub-area, the maximum likelihood posterior ($B_{\text{Bayesian } q_N} = 1.434 \times 10^{-3}$; Figure 7-left, and Equation A9-N) was preponderantly optimized on the prior ($q_{\text{prior}} = 1.272 \times 10^{-3}$; Figure 7-left, and Equation A4). Comparably to the south, CV of the prior was about 2 \times higher than CV of the in-season deletion (Equations A5 and A8-N), but the in-season depletion ($q_N = 3.537 \times 10^{-3}$; Figure 7-left, and Equation A6-N) was weakly distinct (Figure 4). A particular circumstance in the north is that from time to time vessels leave port and fish for a

few hours in the afternoon to evening, catching relatively little but nevertheless counting a full fishing day according to the computational structure of the model.

The MCMC distribution multiplied by average individual weight gave the likelihood distribution of *D. gahi* biomass on day 123 (May 3rd) shown in Figure 7-right, with maximum likelihood and 95% confidence interval of:

$$B_{N \text{ day } 123} = 27,182 \text{ t} \sim 95\% \text{ CI } [20,385 - 94,581] \text{ t} \quad \text{(8-N)}$$

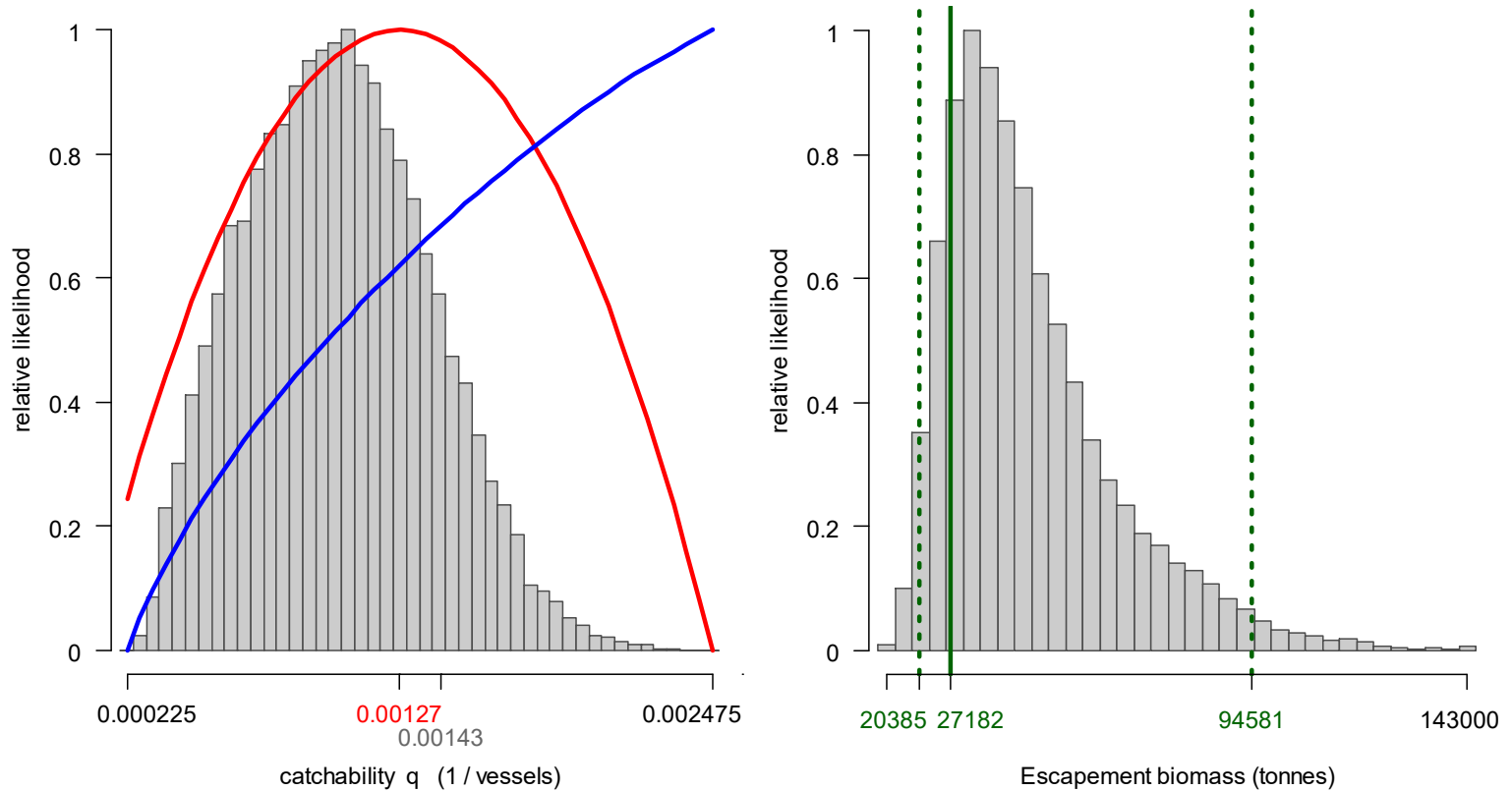


Figure 7. North sub-area. Left: Likelihood distributions for *D. gahi* catchability. Red line: prior model (pre-season survey data), blue line: in-season depletion model, grey bars: combined Bayesian model posterior. Right: Likelihood distribution (grey bars) of escapement biomass, from Bayesian posterior and average individual squid weight at the end of the season. Green lines: maximum likelihood and 95% confidence interval. Note the correspondence to Figure 8.

A relatively unusual pattern in this season was the continuously decreasing function of average individual weight (Figure A1-north).

On the first day of the season estimated *D. gahi* biomass north was 37,635 t \sim 95% CI [25,553 – 126,778] t; statistically higher ($p < 0.03$) than the pre-season estimate of 17,340 t [7,663 – 40,301] (Winter et al. 2023). The highest biomass estimate of the season occurred with the second immigration on day 84, reaching 57,892 t [48,096 – 181,590]. As in the south, the variation of biomass estimate north throughout the season was not statistically significant (Figure 8).

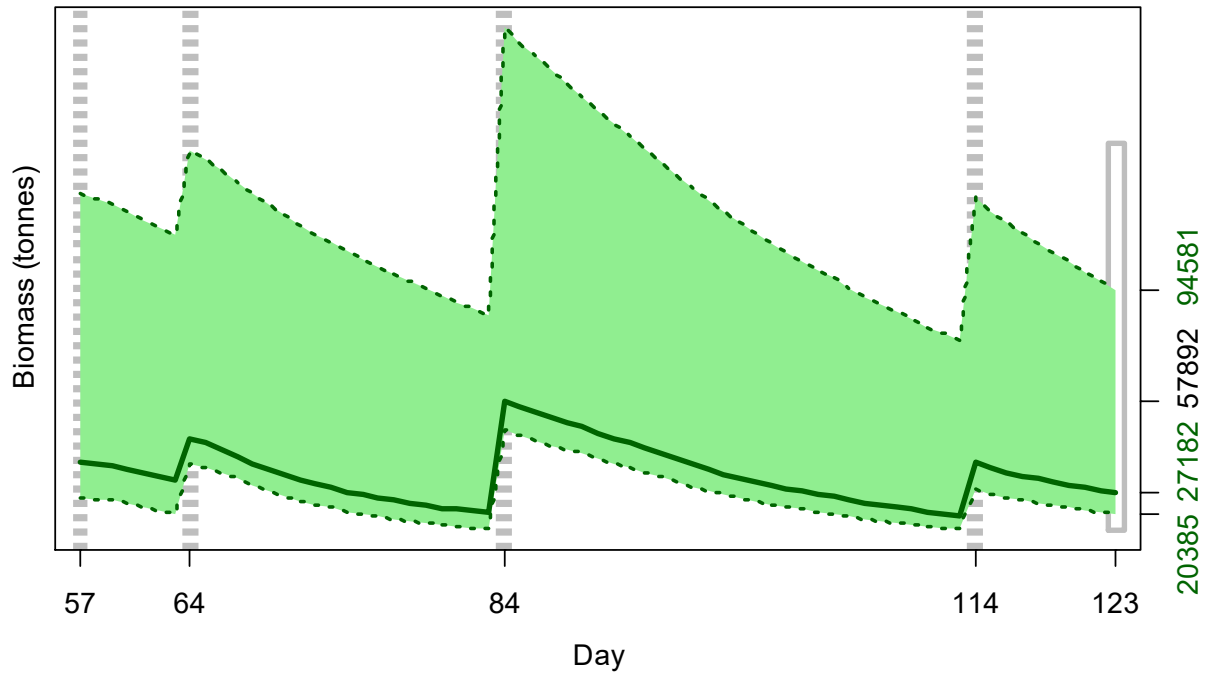


Figure 8. North sub-area. *D. gahi* biomass time series estimated from Bayesian posterior of the depletion model \pm 95% confidence interval. Broken grey bars indicate the start of in-season depletions north; days 57, 64, 84, and 114. Note that the biomass ‘footprint’ on day 123 (May 3rd) corresponds to the right-side plot of Figure 7.

Immigration

Doryteuthis gahi immigration during the season was inferred on each day by how many more squid were estimated present than the day before, minus the number caught and the number expected to have died naturally:

$$\text{Immigration } N_{\text{day } i} = N_{\text{day } i} - (N_{\text{day } i-1} - C_{\text{day } i-1} - M_{\text{day } i-1})$$

where $N_{\text{day } i-1}$ are optimized in the depletion models, $C_{\text{day } i-1}$ calculated as in Equations 2 and 3, and $M_{\text{day } i-1}$ is:

$$M_{\text{day } i-1} = (N_{\text{day } i-1} - C_{\text{day } i-1}) \times (1 - e^{-M})$$

Immigration biomass per day was then calculated as the immigration number per day multiplied by predicted average individual weight from the GAM:

$$\text{Immigration } B_{\text{day } i} = \text{Immigration } N_{\text{day } i} \times \text{GAM } W_{\text{t day } i}$$

All numbers N are themselves derived from the daily average individual weights, therefore the estimation automatically factors in that those squid immigrating on a given day would likely be smaller than average (because younger). Confidence intervals of the immigration estimates were calculated by applying the above algorithms to the MCMC iterations of the depletion models. Resulting total biomasses of *D. gahi* immigration north and south, up to season end (day 123), were:

$$\text{Immigration } B_{\text{S season}} = 49,410 \text{ t} \sim 95\% \text{ CI } [43,207 \text{ to } 143,083] \text{ t} \quad \text{(9-S)}$$

$$\text{Immigration } B_{\text{N season}} = 66,950 \text{ t} \sim 95\% \text{ CI } [52,934 \text{ to } 180,929] \text{ t} \quad \text{(9-N)}$$

Total immigration with randomized addition of the confidence intervals was:

$$\text{Immigration } B_{\text{Total season}} = 116,360 \text{ t} \sim 95\% \text{ CI } [112,010 \text{ to } 278,697] \text{ t} \quad \text{(9-T)}$$

In the south sub-area, the in-season peaks on days 80, 96 and 116 accounted for approximately 16.7%, 49.7% and 30.0% of in-season immigration (start day 57 was de facto not an in-season immigration). In the north sub-area, the in-season peaks on days 64, 84 and 114 accounted for approximately 19.3%, 51.3% and 25.0% of in-season immigration. Both south and north, the remaining immigration percentages were accounted for by the minor fluctuations throughout the season.

Escapement biomass

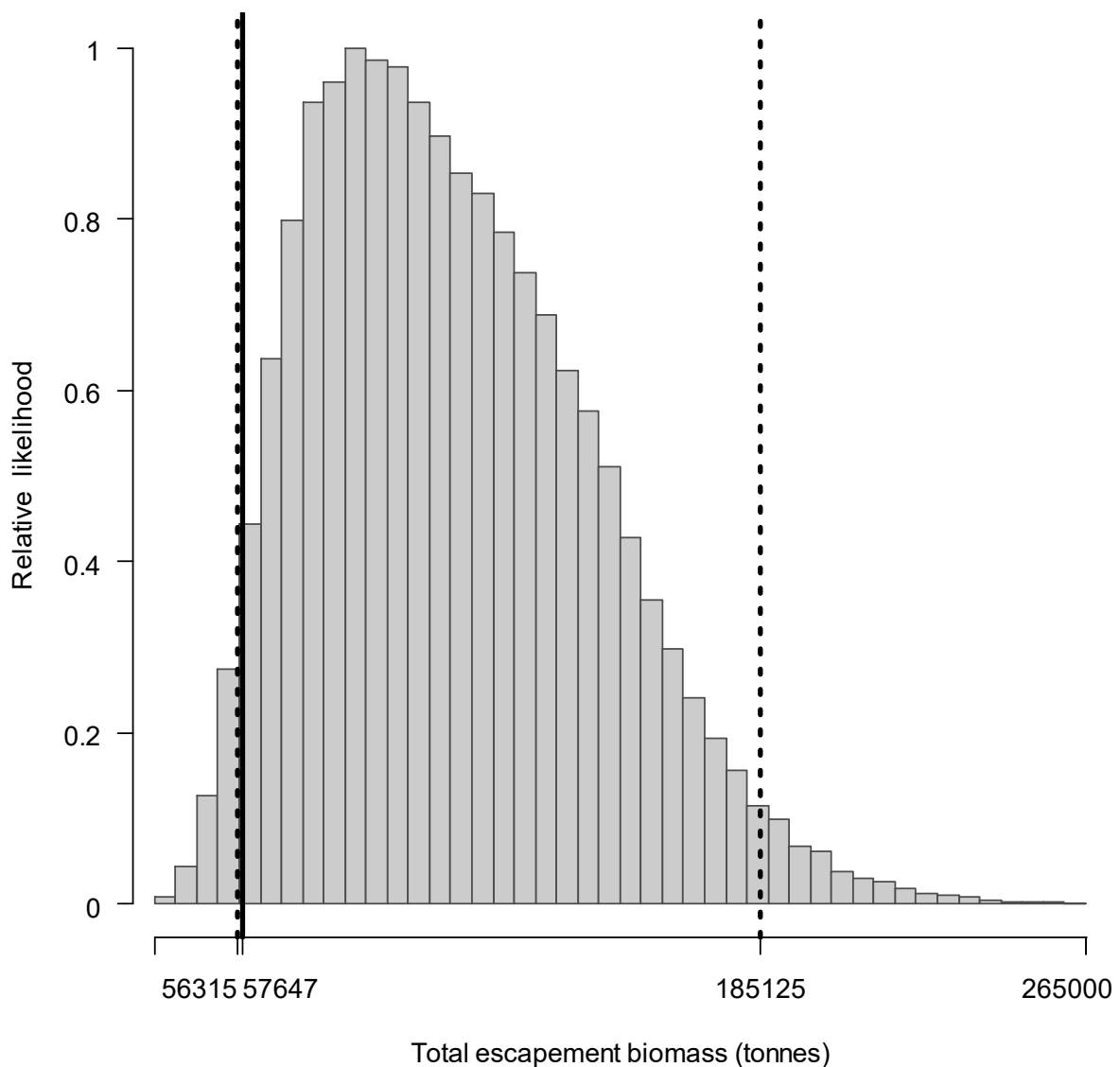


Figure 9 [previous page]. Likelihood distribution with 95% confidence interval of total *D. gahi* escapement biomass at the season end (May 3rd).

Total escapement biomass was defined as the aggregate biomass of *D. gahi* at the end of day 123 (May 3rd) for south and north sub-areas combined (Equations 8). Depletion models are calculated on the inference that all fishing and natural mortality are gathered at mid-day, thus a half day of mortality ($e^{-M/2}$) was added to correspond to the closure of the fishery at 23:59 (mid-night) on May 3rd for the final remaining vessels: Equation 10.

$$\begin{aligned}
 B_{\text{Total day 123}} &= (B_{\text{S day 123}} + B_{\text{N day 123}}) \times e^{-M/2} \\
 &= 58,032 \text{ t} \times 0.99336 \\
 &= 57,647 \text{ t} \sim 95\% \text{ CI } [56,315 - 185,125] \text{ t}
 \end{aligned}
 \tag{10}$$

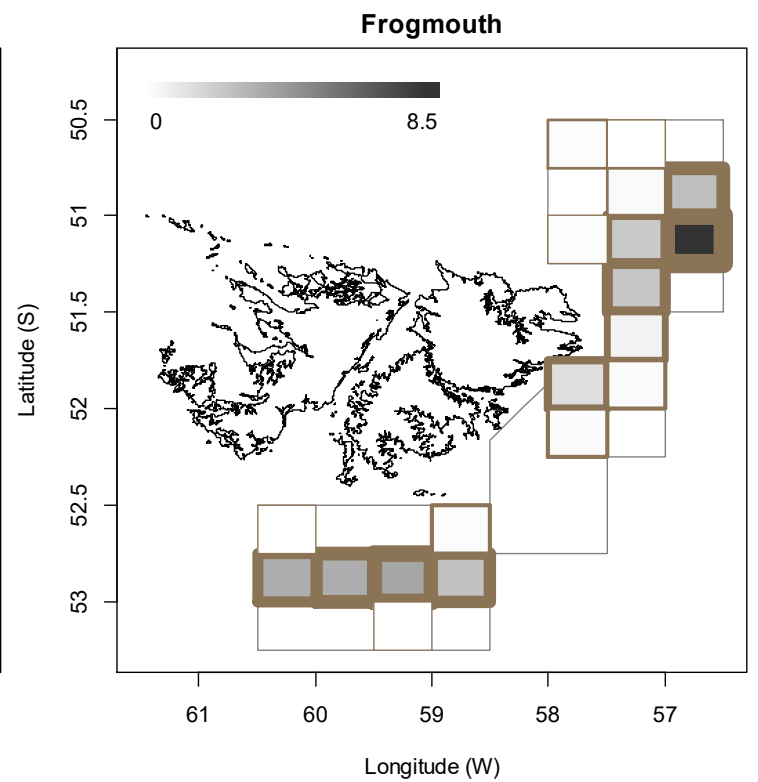
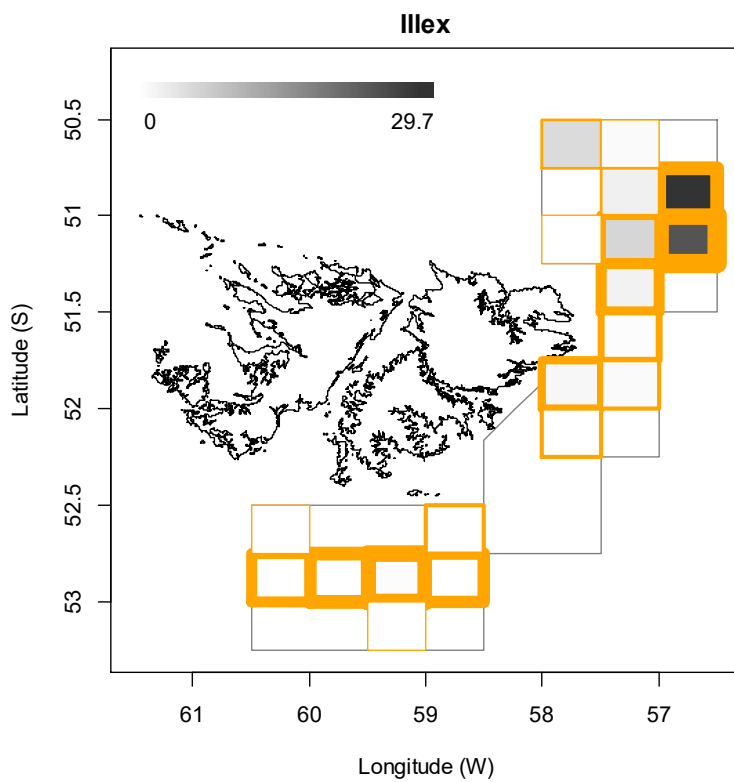
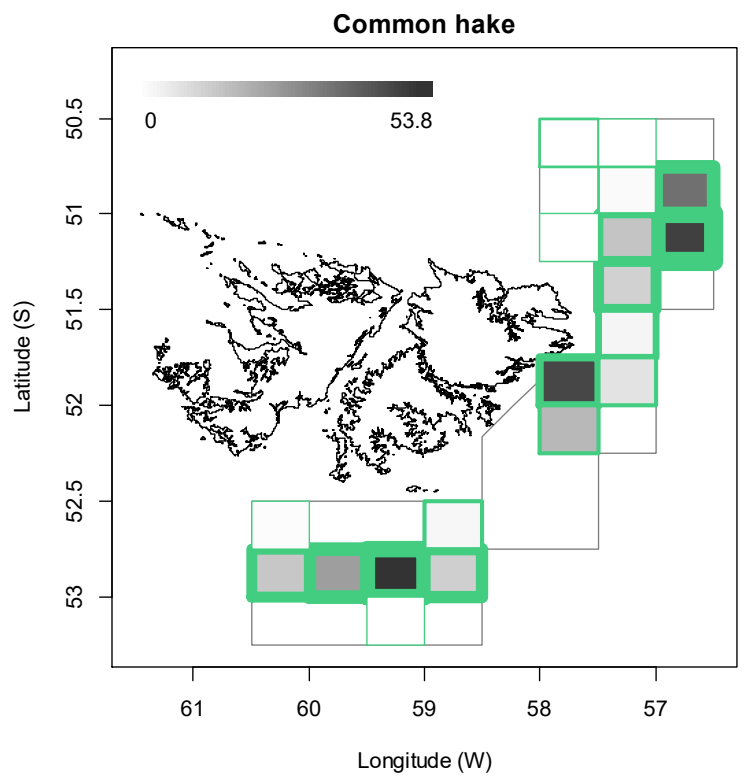
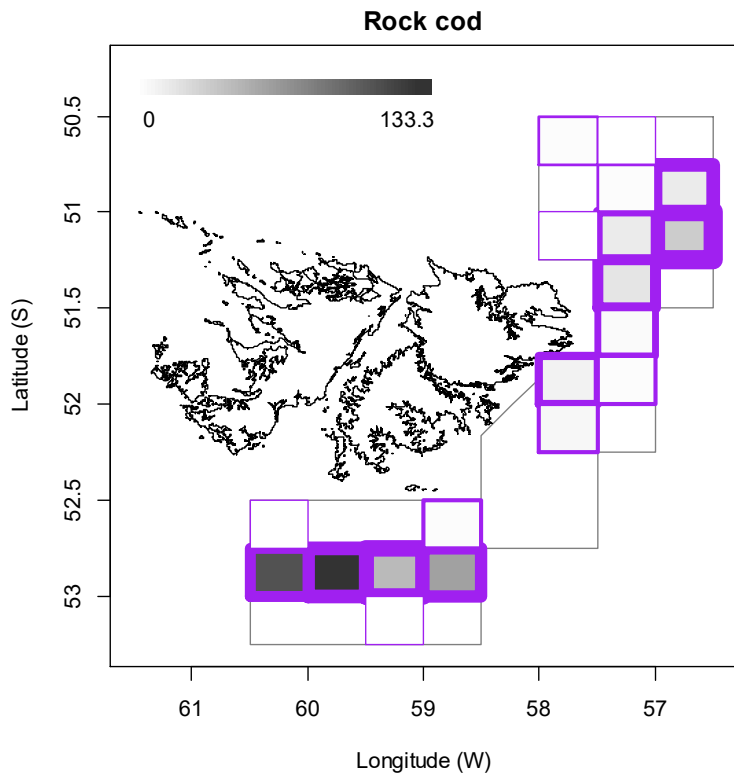
Randomized addition of the south and north distributions gave the aggregate likelihood of total escapement biomass ($B_{\text{Total day 123}}$) shown in Figure 9. With both the south and the north escapement biomass distributions being strongly right-skewed (Figures 5-right and 7-right), the addition of the two produced an extremely asymmetric confidence interval relative to the empirical total. The risk of the fishery in the current season, defined as the proportion of the total escapement biomass distribution below the conservation limit of 10,000 tonnes (Agnew et al. 2002, Barton 2002), was effectively zero. For comparison, the minimum aggregate biomass of the season was estimated on day 79 (March 20th) as 47,984 t \sim 95% CI [47,474 – 162,031] t; also with zero risk of < 10,000 tonnes. The estimated escapement biomass of 57,647 t was the lowest for first seasons since 2020.

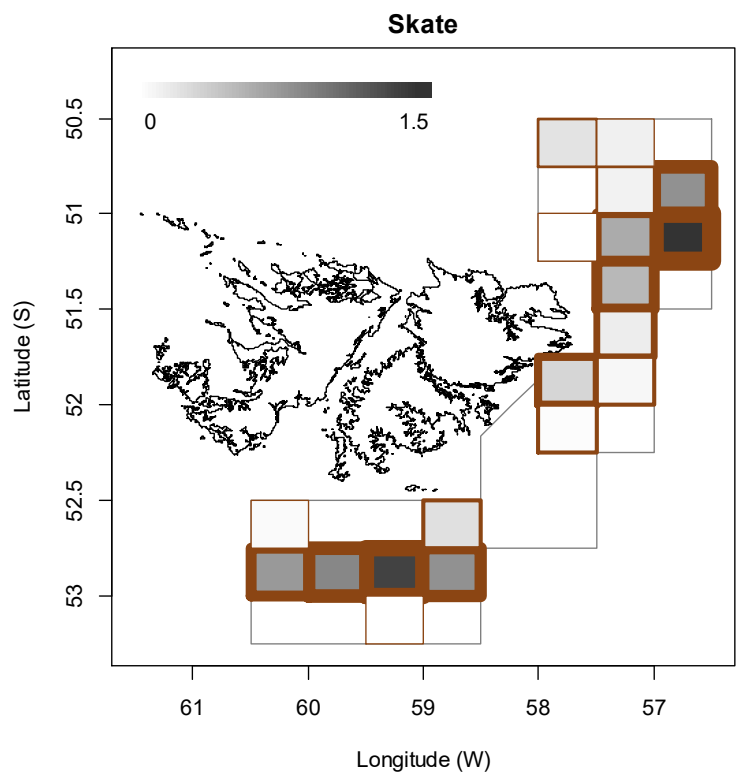
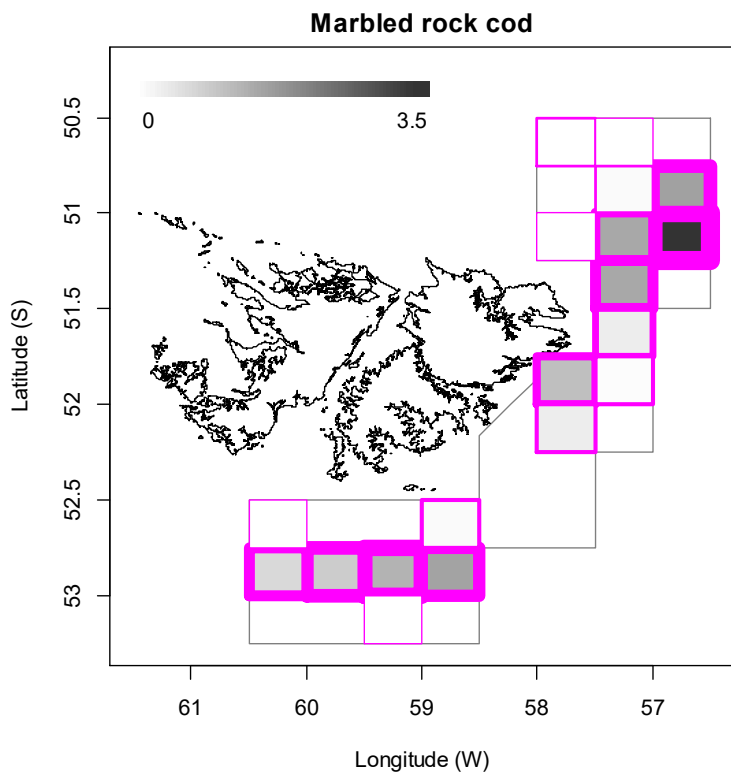
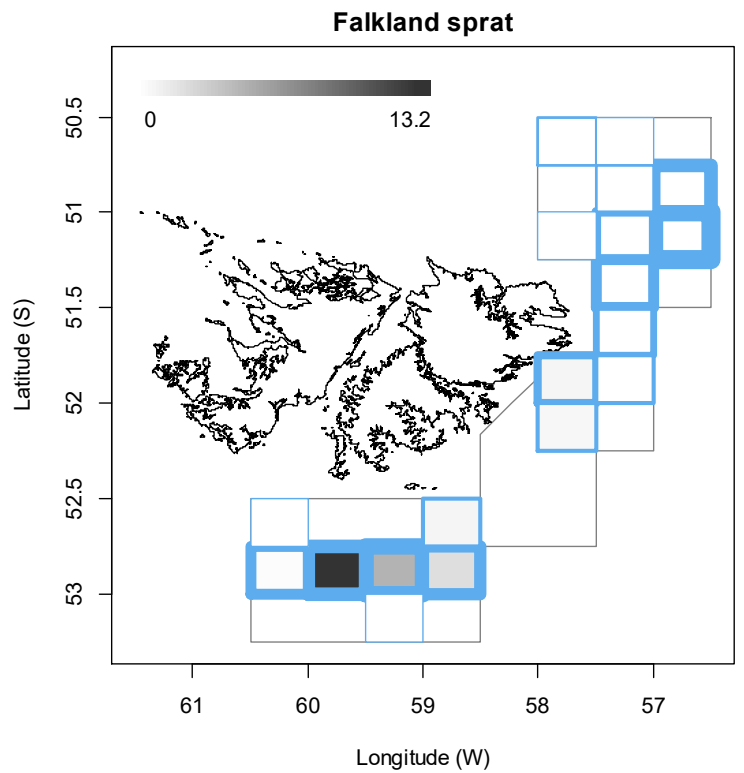
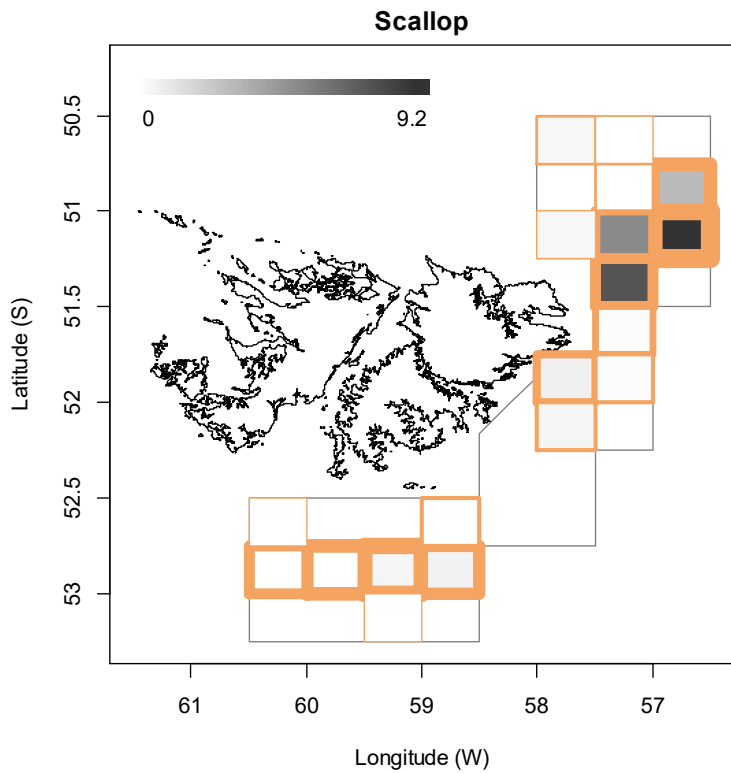
Fishery bycatch

All 972 first-season vessel-days (Table 1) reported *D. gahi* squid as their primary catch. The proportion of season total catch represented by *D. gahi* ($52704367/53666330 = 0.982$; Table A1) was median among first seasons of the past five years. Common hake *Merluccius hubbsi* represented 0.0057 of season total catch ($303532/53666330$; Table A1); the highest proportion in first seasons since 1993 and part of an increasing trend since about 2011. Notwithstanding, hake abundance is generally low around the Falkland Islands during first season, given their migratory timing (Arkhipkin et al. 2012).

Highest aggregate bycatches in first season 2023 were common rock cod *Patagonotothen ramsayi* with 455 tonnes from 955 vessel-days (catch reports), common hake (304 t, 619 v-days), *Illex argentinus* squid (73 t, 416 v-days), frogmouth *Cottoperca gobio* (32 t, 842 v-days), scallops *Zygochlamys* (29 t, 287 v-days), Falkland sprat *Sprattus fuegensis* (22 t, 112 v-days), marbled rock cod *Patagonotothen tessellata* (15 t, 283 v-days), and skates Rajiformes (8 t, 574 v-days). Relative distributions by grid of these bycatches are shown in Figure 10; the complete list of all catches by species is in Table A1.

Figure 10 [below]. Distributions of the eight main bycatches during first season 2023, by noon position grids. Thickness of grid lines is proportional to the number of vessel-days (1 to 206 per grid; 19 different grids were occupied). Grey-scale is proportional to the season bycatch biomass per grid; maximum (tonnes) indicated on each plot.





Trawl area coverage

The impact of bottom trawling on seafloor habitat has been a matter of concern in commercial fisheries (Kaiser et al. 2002; 2006), whereby the potential severity of impact relates to spatial

and temporal extents of trawling (Piet and Hintzen 2012, Gerritsen et al. 2013), as well as the type of trawl gear (Rijnsdorp et al. 2020). For the *D. gahi* fishery, available catch, effort, and positional data are used to summarize the estimated ‘ground’ area coverage^c occupied during the season of trawling.

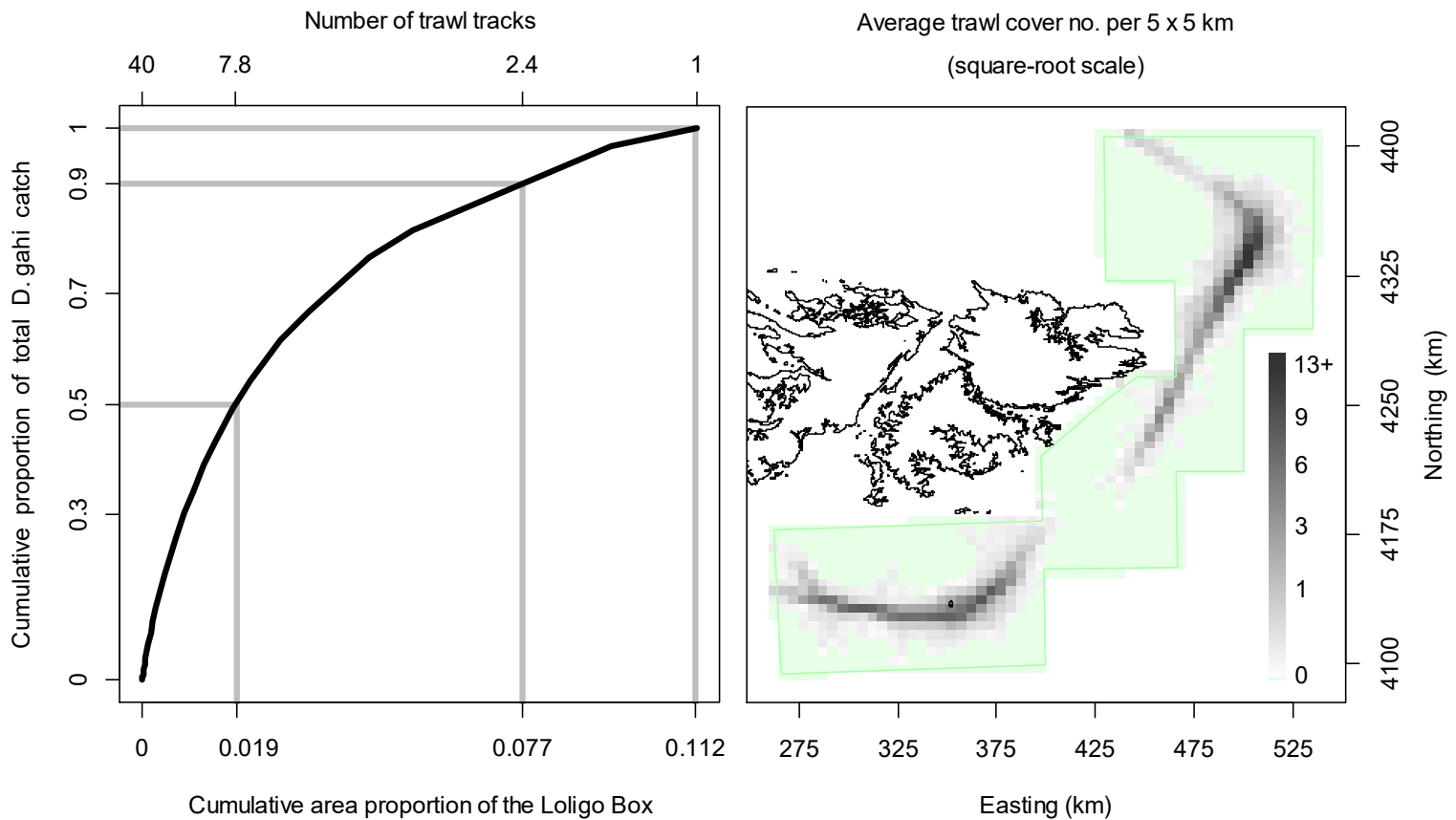


Figure 11. Left: cumulative *D. gahi* catch of 1st season 2023, vs. cumulative area proportion of the Loligo Box the catch was taken from. The maximum number of times that any single area unit was trawled was 40, and catch cumulation by reverse density corresponded approximately to the trawl multiples shown on the top x-axis. Right: trawl cover averaged by 5 × 5 km grid; green area represents zero trawling.

The procedure for summarizing trawl area coverage is described in the Appendix of the second season 2019 report (Winter 2019b). In first season 2023 50% of total *D. gahi* catch was taken from 1.9% of the total area of the Loligo Box, corresponding approximately^d to the aggregate of grounds trawled ≥ 7.8 times. 90% of total *D. gahi* catch was taken from 7.7% of the total area of the Loligo Box, corresponding approximately to the aggregate of grounds trawled ≥ 2.4 times. 100% of total *D. gahi* catch over the season was taken from 11.2% of the total area of the Loligo Box, obviously corresponding to the aggregate of all grounds trawled

^c Appropriate spatial scale for calculating area coverage is a matter of some debate (Amoroso et al. 2018, Kroodsma et al. 2018). Given the comparatively small area of the Loligo Box, a high resolution of 5 km × 5 km was used for these calculations.

^d However, not exactly. There is an expected strong correlation between the density of *D. gahi* catch taken from area units and how often these area units were trawled, but the correlation is not perfectly monotonic.

at least once (Figure 11 - left). The 11.2% total trawl area coverage is just below median among the ten seasons that have been given this analysis so far. Averaged by 5×5 km grid (Figure 11 - right), 6 grids (out of 1383) had coverage of 10 or more (that is to say, every patch of ground within that 5×5 km was on average trawled over 10 times or more). Forty-one grids had coverage of 5 or more, and 92 grids had coverage of 2 or more.

Among the ten seasons given trawl area coverage analysis, all five seasons with above-median CPUE (total *D. gahi* catch divided by total vessel-days) had below-median cumulative area proportion trawled (Figure 12), a statistically significant contrast by permutation test ($p < 0.005$). The contrast suggests a change of state whereby seasons with less abundant catches trawl over wider areas, and vice-versa, although the relationship is not continuous enough for a parametric model (e.g., GLM or GAM).

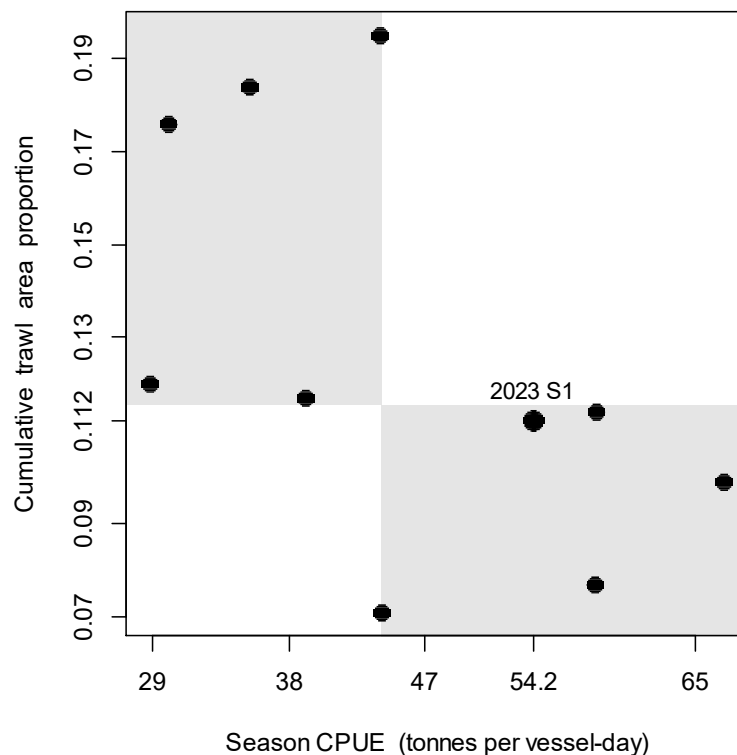


Figure 12. Season CPUEs vs. cumulative trawl area proportions. Opposite median brackets are grey under-shaded. The current season is marked on the plot.

References

- Agnew, D.J., Baranowski, R., Beddington, J.R., des Clers, S., Nolan, C.P. 1998. Approaches to assessing stocks of *Loligo gahi* around the Falkland Islands. *Fisheries Research* 35: 155-169.
- Agnew, D. J., Beddington, J. R., and Hill, S. 2002. The potential use of environmental information to manage squid stocks. *Canadian Journal of Fisheries and Aquatic Sciences*, 59: 1851–1857.
- Akaike, H. 1973. Information theory and an extension of the maximum likelihood principle. 2nd International Symposium on Information Theory: 267-281.

- Amoroso, R.O., Parma, A.M., Pitcher, C.R., McConnaughey, R.A., Jennings, S. 2018. Comment on “Tracking the global footprint of fisheries”. *Science* 361: eaat6713.
- Amukwaya, A. 2023. Observer Report 1355. Technical Document, FIG Fisheries Department. 21 p.
- Arkhipkin, A. 1993. Statolith microstructure and maximum age of *Loligo gahi* (Myopsida: Loliginidae) on the Patagonian Shelf. *Journal of the Marine Biological Association of the UK* 73: 979-982.
- Arkhipkin, A.I., Middleton, D.A.J. 2002. Sexual segregation in ontogenetic migrations by the squid *Loligo gahi* around the Falkland Islands. *Bulletin of Marine Science* 71: 109-127.
- Arkhipkin, A.I., Middleton, D.A.J., Barton, J. 2008. Management and conservation of a short-lived fishery resource: *Loligo gahi* around the Falkland Islands. *American Fisheries Society Symposium* 49: 1243-1252.
- Arkhipkin, A., Brickle, P., Laptikhovskiy, V., Winter, A. 2012. Dining hall at sea: feeding migrations of nektonic predators to the eastern Patagonian Shelf. *Journal of Fish Biology* 81:882–902.
- Arkhipkin, A.I., Hendrickson, L.C., Payá, I., Pierce, G.J., Roa-Ureta, R.H., Robin, J.-P., Winter, A. 2021. Stock assessment and management of cephalopods: advances and challenges for short-lived fishery resources. *ICES Journal of Marine Science* 78: 714-730.
- Barton, J. 2002. Fisheries and fisheries management in Falkland Islands Conservation Zones. *Aquatic Conservation: Marine and Freshwater Ecosystems* 12: 127–135.
- Brooks, S.P., Gelman, A. 1998. General methods for monitoring convergence of iterative simulations. *Journal of computational and graphical statistics* 7:434-455.
- Carlson, J.E. 2014. A generalization of Pythagoras’s theorem and application to explanations of variance contributions in linear models. Research Report No. RR-14-18, Princeton, NJ: Educational Testing Service. 17 p.
- DeLury, D.B. 1947. On the estimation of biological populations. *Biometrics* 3: 145-167.
- FIFD. 2004. Fishery Report, *Loligo gahi*, Second Season 2004. Fishing statistics, biological trends, and stock assessment. Technical Document, Falkland Islands Fisheries Department. 15 p.
- FIG. 2023. Notice 19. Falkland Islands Gazette, Vol. 132, No. 3, 31 March 2023.
- Fournier-Carnoy, L. 2023. Observer Report 1361. Technical Document, FIG Fisheries Dept. 20 p.
- Gamerman, D., Lopes, H.F. 2006. Markov Chain Monte Carlo. Stochastic simulation for Bayesian inference. 2nd edition. Chapman & Hall/CRC.
- Gerritsen, H.D., Minto, C., Lordan, C. 2013. How much of the seabed is impacted by mobile fishing gear? Absolute estimates from Vessel Monitoring System (VMS) point data. *ICES Journal of Marine Science* 70: 523-531.
- Hoenig, J. M. 1982. A compilation of mortality and longevity estimates for fish, mollusks, and cetaceans, with a bibliography of comparative life history studies. University of Rhode Island, Graduate School of Oceanography, Technical Report, 82-2. 14 p.
- Hoenig, J.M. 1983. Empirical use of longevity data to estimate mortality rates. *Fishery Bulletin* 82: 898-903

- Kaiser, M.J., Collie, J.S., Hall, S.J., Jennings, S., Poiner, I.R. 2002. Modification of marine habitats by trawling activities: prognosis and solutions. *Fish and Fisheries* 3: 114-136.
- Kaiser, M.J., Clarke, K.R., Hinz, H., Austen, M.C.V., Somerfield, P.J., Karakassis, I. 2006. Global analysis of response and recovery of benthic biota to fishing. *Marine Ecology Progress Series* 311: 1-14.
- Kroodsma, D.A., Mayorga, J., Hochberg, T., Miller, N.A., Boerder, K., Ferretti, F., Wilson, A., Bergman, B., White, T.D., Block, B.A., Woods, P., Sullivan, B., Costello, C., Worm, B. 2018. Response to Comment on “Tracking the global footprint of fisheries”. *Science* 361: eaat7789.
- Lipiński, M. R. 1979. Universal maturity scale for the commercially important squids (Cephalopoda: Teuthoidea). The results of maturity classification of *Illex illecebrosus* (Le Sueur 1821) population for years 1973–1977. ICNAF Research Document 79/11/38, 40 p.
- MacCall, A.D. 2009. Depletion-corrected average catch: a simple formula for estimating sustainable yields in data-poor situations. *ICES Journal of Marine Science* 66: 2267-2271.
- Magnusson, A., Punt, A., Hilborn, R. 2013. Measuring uncertainty in fisheries stock assessment: the delta method, bootstrap, and MCMC. *Fish and Fisheries* 14: 325-342.
- Nash, J.C., Varadhan, R. 2011. optimx: A replacement and extension of the optim() function. R package version 2011-2.27. <http://CRAN.R-project.org/package=optimx>
- Nicholls, R. 2023. Observer Report 1359. Technical Document, FIG Fisheries Department. 31 p.
- Patterson, K.R. 1988. Life history of Patagonian squid *Loligo gahi* and growth parameter estimates using least-squares fits to linear and von Bertalanffy models. *Marine Ecology Progress Series* 47: 65-74.
- Payá, I. 2006. Fishery Report. *Loligo gahi*, Second Season 2006. Fishery statistics, biological trends, stock assessment and risk analysis. Technical Document, Falkland Islands Fisheries Dept. 40 p.
- Payá, I. 2010. Fishery Report. *Loligo gahi*, Second Season 2009. Fishery statistics, biological trends, stock assessment and risk analysis. Technical Document, Falkland Islands Fisheries Dept. 54 p.
- Peruzzo, M. 2023. Observer Report 1351. Technical Document, FIG Fisheries Department. 26 p.
- Pierce, G.J., Guerra, A. 1994. Stock assessment methods used for cephalopod fisheries. *Fisheries Research* 21: 255–285.
- Piet, G.J., Hintzen, N.T. 2012. Indicators of fishing pressure and seafloor integrity. *ICES Journal of Marine Science* 69: 1850-1858.
- Plet-Hansen, K.S., Larsen, E., Mortensen, L.O., Nielsen, J.R., Ulrich, C. 2018. Unravelling the scientific potential of high-resolution fishery data. *Aquatic Living Resources* 31:24.
- Punt, A.E., Hilborn, R. 1997. Fisheries stock assessment and decision analysis: the Bayesian approach. *Reviews in Fish Biology and Fisheries* 7:35-63.
- Rijnsdorp, A.D., Hiddink, J.G., van Denderen, P.D., Hintzen, N.T., Eigaard, O.R., Valanko, S., Bastardie, F., Bolam, S.G., Boulcott, P., Egekvist, J., Garcia, C., van Hoey, G., Jonsson, P., Laffargue, P., Nielsen, J.R., Piet, G.J., Sköld, M., van Kooten, T. 2020. Different bottom trawl fisheries have a differential impact on the status of the North Sea seafloor habitats. *ICES Journal of Marine Science* 77: 1772–1786.

- Roa-Ureta, R. 2012. Modelling in-season pulses of recruitment and hyperstability-hyperdepletion in the *Loligo gahi* fishery around the Falkland Islands with generalized depletion models. ICES Journal of Marine Science 69: 1403–1415.
- Roa-Ureta, R., Arkhipkin, A.I. 2007. Short-term stock assessment of *Loligo gahi* at the Falkland Islands: sequential use of stochastic biomass projection and stock depletion models. ICES Journal of Marine Science 64: 3-17.
- Rosenberg, A.A., Kirkwood, G.P., Crombie, J.A., Beddington, J.R. 1990. The assessment of stocks of annual squid species. Fisheries Research 8: 335-350.
- Shaw, P.W., Arkhipkin, A.I., Adcock, G.J., Burnett, W.J., Carvalho, G.R., Scherbich, J.N., Villegas, P.A. 2004. DNA markers indicate that distinct spawning cohorts and aggregations of Patagonian squid, *Loligo gahi*, do not represent genetically discrete subpopulations. Marine Biology, 144: 961-970.
- Swartzman, G., Huang, C., Kaluzny, S. 1992. Spatial analysis of Bering Sea groundfish survey data using generalized additive models. Canadian Journal of Fisheries and Aquatic Sciences 49: 1366-1378.
- Winter, A. 2019a. Stock assessment – Falkland calamari *Doryteuthis gahi* 1st season 2019. Technical Document, Falkland Islands Fisheries Department. 37 p.
- Winter, A. 2019b. Stock assessment – Falkland calamari *Doryteuthis gahi* 2nd season 2019. Technical Document, Falkland Islands Fisheries Department. 36 p.
- Winter, A. 2021. Stock assessment – Falkland calamari *Doryteuthis gahi* 1st season 2021. Technical Document, Falkland Islands Fisheries Department. 34 p.
- Winter, A., Skeljo, F. 2022. Stock assessment – Falkland calamari *Doryteuthis gahi* 1st season 2022. Technical Document, Falkland Islands Fisheries Department. 30 p.
- Winter, A., Arkhipkin, A. 2015. Environmental impacts on recruitment migrations of Patagonian longfin squid (*Doryteuthis gahi*) in the Falkland Islands with reference to stock assessment. Fisheries Research 172: 85-95.
- Winter, A., Raczynski, M., Peruzzo, M. 2023. Falkland calamari (*Doryteuthis gahi*) 1st pre-season 2023 stock assessment survey. Technical Document, Falkland Islands Fisheries Department. 17 p.

Appendix
***Doryteuthis gahi* individual weights**

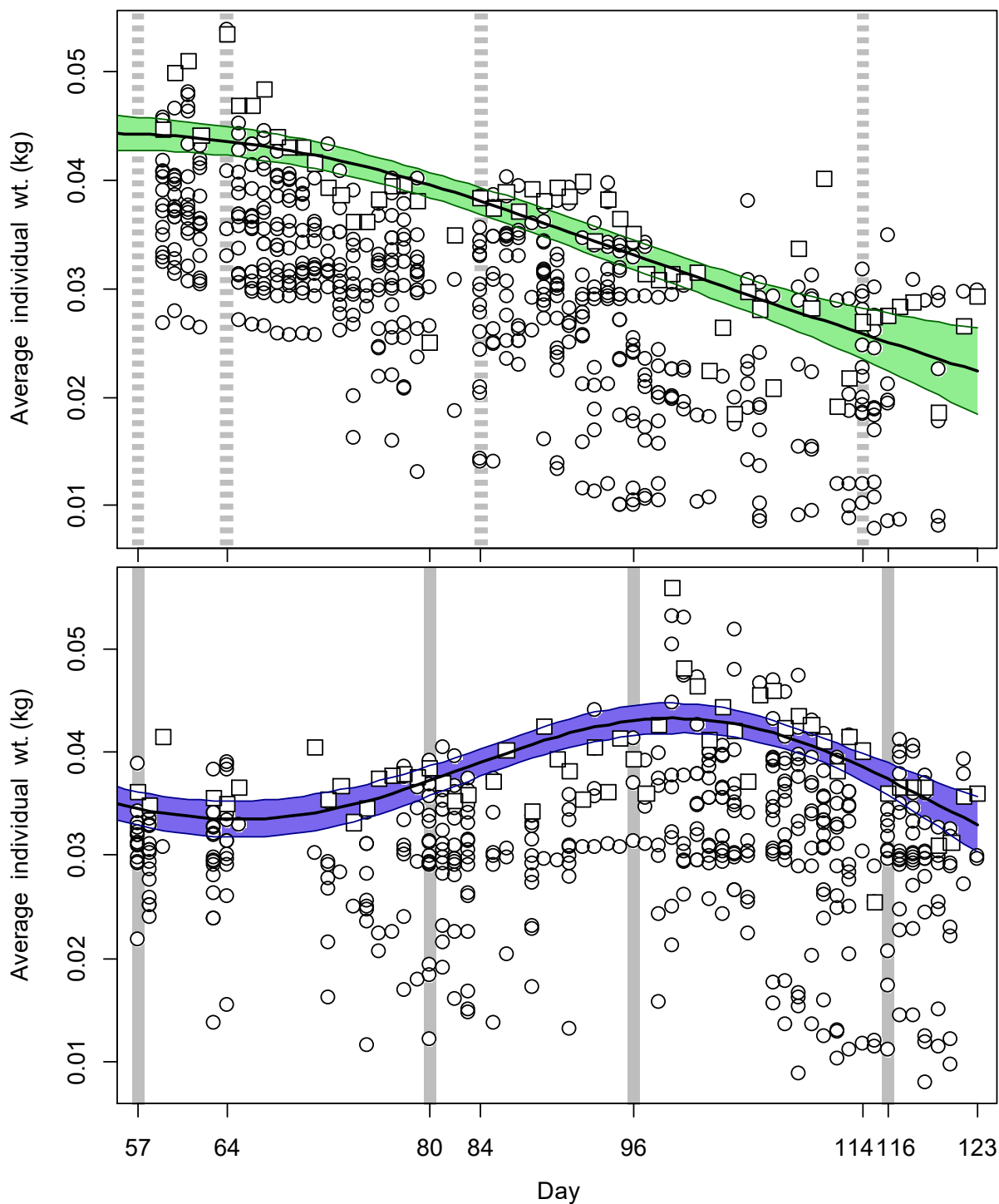


Figure A1. North (top) and south (bottom) sub-area daily average individual *D. gahi* weights from commercial size categories per vessel (circles) and observer measurements (squares). GAMs of the daily trends \pm 95% confidence interval (centre lines and colour under-shading).

To smooth fluctuations, GAM trends were calculated of daily average individual weights. North and south sub-areas were calculated separately. For continuity, GAMs were calculated using all pre-season survey and in-season data contiguously. North and south GAMs were first

calculated separately on the commercial and observer data. As full observer coverage in the *D. gahi* fishery has now become standard, observer data GAMs were taken as the baseline trends, augmented by the margin by which commercial data are more frequent than observer data (if at all). For example, this season had 972 commercial fishing days (Table 1), and 940 observer days (FIG + contract observers). The final GAM trend was therefore calculated as:

$$\text{GAM}_{\text{Wt}} = \text{Obs GAM}_{\text{Wt}} - \left(1 - \text{pmin}\left(1, \frac{940}{972}\right)\right) \times \text{mean}(\text{Obs GAM}_{\text{Wt}} - \text{Comm GAM}_{\text{Wt}})$$

As before, inclusion of both GAMs effected that the greater day-to-day consistency of the commercial data trends, and the greater point value accuracy of the observer data, are represented in the calculations. GAM plots of the north and south sub-areas are in Figure A1.

Prior estimates and CV

The pre-season survey had estimated *D. gahi* biomass of 44,015 tonnes (Winter et al. 2023). Hierarchical bootstrapping of the inverse distance weighting algorithm obtained a coefficient of variation (CV) equal to 21.8% of the survey biomass distribution. From modelled survey catchability, Payá (2010) had estimated average net escapement of up to 22%, which was added to the CV:

$$44,015 \pm (.218 + .22) = 44,015 \pm 43.8\% = 44,015 \pm 19,277 \text{ t} \quad (\text{A1})$$

The 22% escapement was added as a linear increase in the variability, but was not used to reduce the total estimate, because squid that escape one trawl are likely to be part of the biomass concentration that is available to the next trawl.

D. gahi numbers from the survey were estimated as the survey biomasses divided by the GAM-predicted individual weight average for the survey: 0.0418 kg. The average coefficient of variation (CV) of the GAM over the duration of the pre-season survey was 2.7%, and CV of the length-weight conversion relationship (Equation 7) was 13.9%. Joining these sources of variation with the pre-season survey biomass estimates and individual weight averages (above) gave estimated *D. gahi* numbers at survey end (day 52) of:

$$\begin{aligned} \text{prior } N_{\text{day } 52} &= \frac{44,015 \times 1000}{0.0418} \pm \sqrt{43.8\%^2 + 2.7\%^2 + 13.9\%^2} \\ &= 1.054 \times 10^9 \pm 46.0\% \end{aligned} \quad (\text{A2})$$

The combined catchability coefficient (q) prior was taken on day 57, the first day of the season, when 15 vessels fished in the south sub-area and no vessels fished in the north sub-area (15 total; Figure 2). Abundance on day 57 was discounted for natural mortality over the 5 days since the end of the survey:

$$\text{prior } N_{\text{day } 57} = \text{prior } N_{\text{day } 52} \times e^{-M \cdot (57 - 52)} - \text{CNMD}_{\text{day } 57} = 0.986 \times 10^9 \quad (\text{A3})$$

where $\text{CNMD}_{\text{day } 57} = 0$ as no catches intervened between the end of the survey and the start of commercial season. Thus:

$$\text{prior } q = \text{C(N)}_{\text{day } 57} / (\text{prior } N_{\text{day } 57} \times E_{\text{day } 57})$$

$$\begin{aligned}
&= (C(B)_{\text{day } 57} / Wt_{\text{day } 57}) / (\text{prior } N_{\text{day } 57} \times E_{\text{day } 57}) \\
&= (770.5 \text{ t} / 0.0410 \text{ kg}) / (0.986 \times 10^9 \times 15 \text{ vessel-days}) \\
&= 1.272 \times 10^{-3} \text{ vessels}^{-1} \text{ e} \tag{A4}
\end{aligned}$$

SD_{prior q} (Equation 4) was calculated as prior q multiplied by its CV. CV_{prior q} was calculated as the sum of variability in prior N_{day 52} (Equation A2) plus variability in the catches of vessels on start day 57, plus variability of the natural mortality (see Appendix section Natural mortality).

$$\begin{aligned}
CV_{\text{prior } q} &= \sqrt{46.0\%^2 + \left(\frac{SD(C(B)_{\text{vessels day } 57})}{\text{mean}(C(B)_{\text{vessels day } 57})} \right)^2 + (1 - (1 - CV_M)^{(57 - \text{mid_survey}}))^2} \\
&= \sqrt{46.0\%^2 + 25.6\%^2 + 100.0\%^2} = 113.0\%
\end{aligned}$$

$$SD_{\text{prior } q} = \text{prior } q \times CV_{\text{prior } q} = 1.437 \times 10^{-3} \text{ vessels}^{-1} \tag{A5}$$

Depletion model estimates and CV

For the south sub-area, the equivalent of Equation 2 with four N_{day} was optimized on the difference between predicted and actual catches (Equation 3), resulting in parameters values:

$$\begin{aligned}
\text{depletion } N1_{S \text{ day } 57} &= 0.857 \times 10^9; & \text{depletion } N2_{S \text{ day } 80} &= 0.205 \times 10^9 \\
\text{depletion } N3_{S \text{ day } 96} &= 0.508 \times 10^9; & \text{depletion } N4_{S \text{ day } 116} &= 0.362 \times 10^9 \\
\text{depletion } Q_S &= 1.802 \times 10^{-3} \text{ f} \tag{A6-S}
\end{aligned}$$

The normalized root-mean-square deviation of predicted vs. actual catches was calculated as the CV of the model:

$$\begin{aligned}
CV_{\text{rmsd } S} &= \frac{\sqrt{\sum_{i=1}^n (\text{predicted } C(N)_{S \text{ day } i} - \text{actual } C(N)_{S \text{ day } i})^2 / n}}{\text{mean}(\text{actual } C(N)_{S \text{ day } i})} \\
&= 2.441 \times 10^6 / 8.671 \times 10^6 = 28.2\% \tag{A7-S}
\end{aligned}$$

CV_{rmsd S} was added to the variability of the GAM-predicted individual weight averages for the season (Figure A1-S); equal to a CV of 2.06% south. CVs of the depletion were then calculated as the sum:

$$\begin{aligned}
CV_{\text{depletion } S} &= \sqrt{CV_{\text{rmsd } S}^2 + CV_{\text{GAM } Wt S}^2} = \sqrt{28.2\%^2 + 2.06\%^2} \\
&= 28.2\% \tag{A8-S}
\end{aligned}$$

^e On Figure 5-left and Figure 7-left.

^f On Figure 5-left.

For the north sub-area, the Equation 2 equivalent with four N_{day} was optimized on the difference between predicted and actual catches (Equation 3), resulting in parameter values:

$$\begin{aligned}
 \text{depletion } N1_{N \text{ day } 57} &= 0.363 \times 10^9; & \text{depletion } N2_{N \text{ day } 64} &= 0.279 \times 10^9 \\
 \text{depletion } N3_{N \text{ day } 84} &= 0.632 \times 10^9; & \text{depletion } N2_{N \text{ day } 114} &= 0.373 \times 10^9 \\
 \text{depletion } q_N &= 3.537 \times 10^{-3} \text{ g} & &
 \end{aligned}
 \tag{A6-N}$$

Root-mean-square deviation of predicted vs. actual catches was calculated as the CV of the model:

$$\begin{aligned}
 CV_{\text{rmsd } N} &= \frac{\sqrt{\sum_{i=1}^n (\text{predicted } C(N)_{N \text{ day } i} - \text{actual } C(N)_{N \text{ day } i})^2 / n}}{\text{mean}(\text{actual } C(N)_{N \text{ day } i})} \\
 &= 6.693 \times 10^6 / 12.174 \times 10^6 = 55.0\%
 \end{aligned}
 \tag{A7-N}$$

$CV_{\text{rmsd } N}$ was added to the variability of the GAM-predicted individual weight averages for the season (Figure A1-N); equal to a CV of 2.60% north. CVs of the depletion were then calculated as the sum:

$$\begin{aligned}
 CV_{\text{depletion } N} &= \sqrt{CV_{\text{rmsd } N}^2 + CV_{\text{GAM } Wt \text{ } N}^2} = \sqrt{55.0\%^2 + 2.60\%^2} \\
 &= 55.0\%
 \end{aligned}
 \tag{A8-N}$$

Combined Bayesian models

For the south sub-area, joint optimization of Equations 3 and 4 resulted in parameters values:

$$\begin{aligned}
 \text{Bayesian } N1_{S \text{ day } 57} &= 1.048 \times 10^9; & \text{Bayesian } N2_{S \text{ day } 80} &= 0.228 \times 10^9 \\
 \text{Bayesian } N3_{S \text{ day } 96} &= 0.589 \times 10^9; & \text{Bayesian } N2_{S \text{ day } 116} &= 0.411 \times 10^9 \\
 \text{Bayesian } q_S &= 1.443 \times 10^{-3} \text{ h} & &
 \end{aligned}
 \tag{A9-S}$$

These parameters produced the fit between predicted catches and actual catches shown in Figure A2-S.

For the north sub-area, joint optimization of Equations 3 and 4 resulted in parameters values:

$$\begin{aligned}
 \text{Bayesian } N1_{N \text{ day } 57} &= 0.850 \times 10^9; & \text{Bayesian } N2_{N \text{ day } 64} &= 0.323 \times 10^9 \\
 \text{Bayesian } N3_{N \text{ day } 84} &= 0.986 \times 10^9; & \text{Bayesian } N2_{N \text{ day } 114} &= 0.710 \times 10^9 \\
 \text{Bayesian } q_N &= 1.434 \times 10^{-3} \text{ i} & &
 \end{aligned}
 \tag{A9-N}$$

These parameters produced the fit between predicted catches and actual catches shown in Figure A2-N.

^g Off the scale on Figure 7-left.

^h On Figure 5-left.

ⁱ On Figure 7-left.

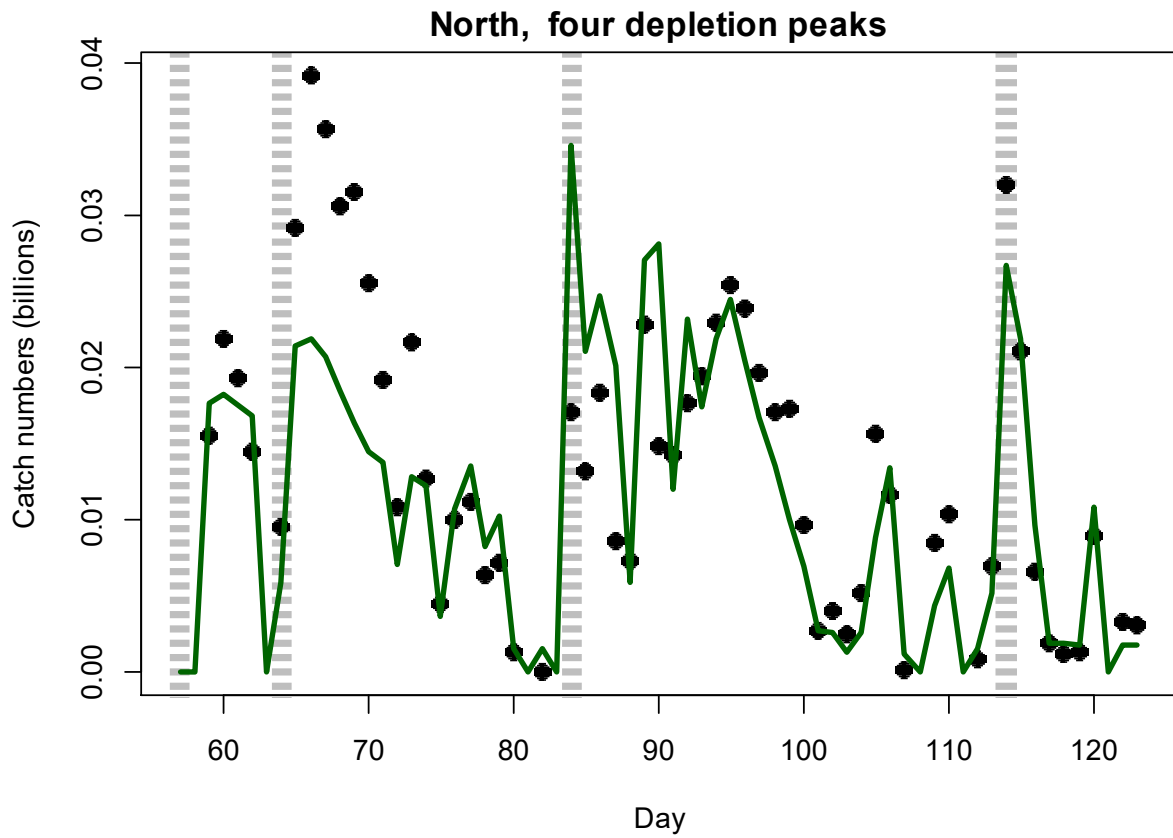
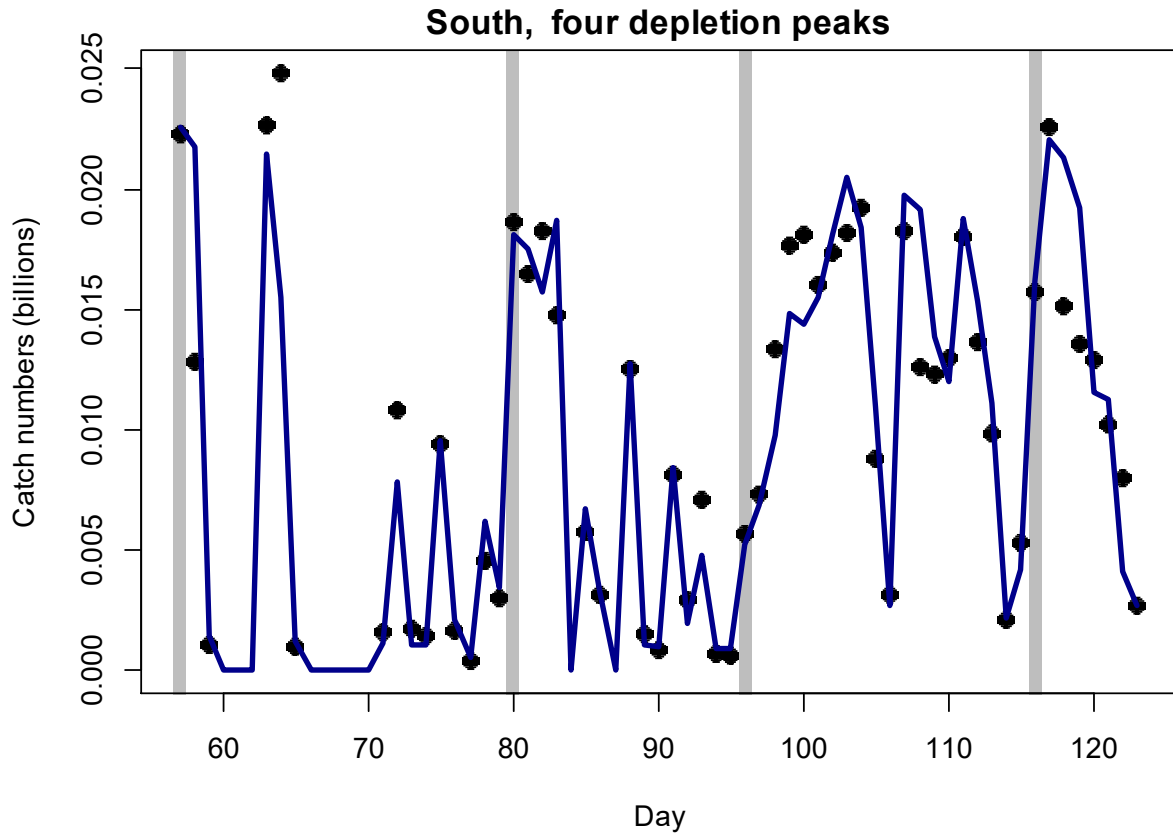


Figure A2-S [previous page top]. Daily catch numbers estimated from actual catch (black points) and predicted from the depletion model (purple line) in the south sub-area.

Figure A2-N [previous page bottom]. Daily catch numbers estimated from actual catch (black points) and predicted from the depletion model (green line) in the north sub-area.

Natural mortality

Natural mortality is parameterized as a constant instantaneous rate $M = 0.0133 \text{ day}^{-1}$ (Roa-Ureta and Arkhipkin 2007), based on Hoenig's (1983) log mortality vs. log maximum age regression, applied to an estimated maximum age of 352 days for *D. gahi*:

$$\begin{aligned} \log(M) &= 1.44 - 0.982 \times \log(\text{age}_{\max}) \\ M &= \exp(1.44 - 0.982 \times \log(352)) \\ &= 0.0133 \end{aligned} \tag{A10}$$

Hoenig (1983) derived Equation A10 from the regression of 134 stocks among 79 species of fish, molluscs, and cetaceans. Hoenig's regression obtained $R^2 = 0.82$, but a corresponding coefficient of variation (CV) was not published. The CV is estimated by re-computing the regression from original data in Hoenig (1982)^j, extracting the standard error (σ), and calculating the CV from the equation:

$$CV = (\exp(\sigma^2) - 1)^{1/2} \quad (\text{MacCall 2009})$$

which gave

$$CV_M = (\exp(0.472^2) - 1)^{1/2} = 49.96\% \tag{A11}$$

MacCall (2009) suggested that CV_M should be assumed a minimum of 0.5, effectively equivalent to Equation A11.

CV_M was aggregated over the number of days between the midpoint of the survey and the commercial season start, rather than between the end of the survey and commercial season start, as the midpoint more accurately reflects how much time has elapsed since the fishing area on average was surveyed. The midpoint of the survey was calculated as the mean day weighted by the number of survey trawls taken per day:

$$\text{mid_survey} = \frac{\sum(\text{day} \times N_{\text{survey trawls}}|_{\text{day}})}{\sum(N_{\text{survey trawls}}|_{\text{day}})} = 44.4^k \tag{A12}$$

CV_M was thus further indexed by $1 - (1 - CV_M)$ to ensure that the value could not decrease if CV_M was hypothetically $> 100\%$:

$$1 - (1 - CV_M)^{(\text{commercial season start} - \text{mid_survey})} \tag{A13}$$

Equation A13 is included in Equation A5.

^j Hoenig (1982) listed 130 rather than 134 stocks, but these obtained the same parameters of 1.44 and -0.982 .

^k In common nomenclature day 44 is February 13th.

Total catch by species

Table A1: Total reported catches and discard by taxon during first season 2023 C-license fishing, and number of catch reports (vessel-days) in which each taxon occurred. Does not include incidental catches of pinnipeds or seabirds.

Species Code	Species / Taxon	Catch Wt. (KG)	Discard Wt. (KG)	N Reports
LOL	<i>Doryteuthis gahi</i>	52704367	62575	972
PAR	<i>Patagonotothen ramsayi</i>	455353	451254	955
HAK	<i>Merluccius hubbsi</i>	303532	33817	619
ILL	<i>Illex argentinus</i>	73479	5614	416
CGO	<i>Cottoperca gobio</i>	31813	31633	842
SCA	<i>Zygochlamys patagonica</i>	28603	28517	287
SAR	<i>Sprattus fuegensis</i>	22412	22312	112
PTE	<i>Patagonotothen tessellata</i>	14601	14577	283
RAY	Rajiformes	8333	8136	574
BAC	<i>Salilota australis</i>	5491	1603	141
TOO	<i>Dissostichus eleginoides</i>	3856	3826	284
DGH	<i>Schroederichthys bivius</i>	3302	3302	348
SAA	<i>Salmo trutta</i>	2350	2350	7
OCT	<i>Octopus spp.</i>	1991	1991	239
ING	<i>Moroteuthis ingens</i>	1486	1481	164
KIN	<i>Genypterus blacodes</i>	1246	1035	120
MED	Medusae sp.	640	640	39
BLU	<i>Micromesistius australis</i>	630	630	27
CHE	<i>Champscephalus esox</i>	579	579	63
LIM	<i>Lithodes murrayi</i>	435	435	34
ALF	<i>Allothunnus fallai</i>	420	420	49
GRV	<i>Macrourus spp.</i>	372	372	31
LIT	<i>Lithodes turkayi</i>	239	239	20
UCH	Sea urchin	163	163	21
RED	<i>Sebastes oculatus</i>	123	123	22
GRF	<i>Coelorhynchus fasciatus</i>	102	102	7
DGS	<i>Squalus acanthias</i>	93	93	10
MAR	<i>Martialia hyadesi</i>	61	61	7
POR	<i>Lamna nasus</i>	40	40	1
WHI	<i>Macruronus magellanicus</i>	33	33	12
PAF	<i>Paralomis formosa</i>	31	31	3
MUL	<i>Eleginops maclovinus</i>	26	26	11
MUN	<i>Grimothea gregaria</i>	24	24	2
LIS	<i>Lithodes santolla</i>	22	22	2
SEP	<i>Seriolella porosa</i>	22	22	5
BUT	<i>Stromateus brasiliensis</i>	20	20	3
PAT	<i>Merluccius australis</i>	14	14	3
MYX	<i>Myxine spp.</i>	10	10	6
CRB	Crab	9	9	2
ANI	<i>Champscephalus gunnari</i>	4	4	1
BDU	<i>Brama dussumieri</i>	2	2	1
EEL	<i>Iluocoetes fimbriatus</i>	1	1	1
Total		53666330	678138	972